

# 3-manifolds having complexity at most 9

Bruno MARTELLI      Carlo PETRONIO

November 29, 2018

## Contents

<b>1</b>	<b>Complexity theory and an overview of the algorithm</b>	<b>3</b>
1.1	Complexity theory . . . . .	3
1.2	Loops and moves . . . . .	5
1.3	The main algorithm . . . . .	6
1.4	Splitting of a minimal spine into bricks . . . . .	8
1.5	The input for the main algorithm: an algorithm which finds the bricks	11
1.6	Main results up to complexity 9 . . . . .	12
<b>2</b>	<b>Surfaces and transverse surfaces in a spine</b>	<b>15</b>
2.1	Disconnecting surfaces . . . . .	15
2.2	A criterion for non-minimality . . . . .	16
2.3	Simply transverse surfaces . . . . .	17
2.4	Co-disconnecting surfaces . . . . .	21
<b>3</b>	<b>Intrinsic definition of bricks and assembling</b>	<b>22</b>
3.1	Loop-triod-systems . . . . .	22
3.2	Assembling . . . . .	24
3.3	Bricks and bases . . . . .	27
<b>4</b>	<b>Splitting of a minimal spine into bricks</b>	<b>28</b>
<b>5</b>	<b>Properties of bricks</b>	<b>35</b>
5.1	Evolution of traces . . . . .	36
5.2	Free traces with 2 and 4 vertices in a brick . . . . .	40
5.3	Further properties . . . . .	50

<b>6 Bases of bricks for <math>n \leq 9</math></b>	<b>55</b>
6.1 Twists . . . . .	56
6.2 The set $\mathcal{B}_n^0$ for $n \leq 9$ . . . . .	61

## Introduction

This paper is devoted to the theoretical description and illustration of results of an algorithm which has enabled us to give a complete list, without repetitions, of all closed oriented irreducible 3-manifolds of complexity up to 9. More interestingly, we have actually been able to give a “name” to each such manifold, *i.e.* to recognize its canonical decomposition into Seifert fibered spaces and hyperbolic manifolds already considered by other authors. The complexity we are referring to here is that introduced by Matveev ([4], see also [3]), given by the minimal number of vertices of a standard spine (this has been proved in [4] to be equal to the minimal number of tetrahedra in a triangulation).

Our algorithm relies on several purely topological structural results which we prove about the set of minimal spines. Before sketching these results, we mention our most interesting experimental discoveries about complexity 9 (recall that it was already known to Matveev [4] that up to complexity 8 all manifolds are graph-manifolds; tables up to complexity 6 are in [5], and up to 7 in [7]). First, we can show that there are 1156 manifolds of complexity 9, 272 of them are lens spaces, 863 are more general graph-manifolds which do not contain non-separating tori, 17 of them are torus bundles over  $S^1$ , 10 of them are graph-manifolds with graph  $\bigcirc \rightarrow$ , and there are also 4 closed hyperbolic manifolds. More importantly, these 4 manifolds turn out to be precisely those of least known volume, in accordance with the ideas about complexity and volume stated in [3].

We turn now to a more punctual description of our topological results, starting from their motivation. Knowing what the complexity of a manifold exactly is (see Subsections 1.1 and 1.2), it is not so hard to devise a general scheme for an algorithm listing all manifolds of a given complexity  $n$  (see Subsection 1.3). However, three main issues arise: (1) *minimality*: find criteria for non-minimality flexible enough to guarantee that if a spine with  $n$  vertices is non-minimal then it satisfies one of the criteria; (2) *recognition*: find invariants which allow to give each manifold of complexity  $n$  a name, or at least to guarantee that the final list of manifolds contains no duplicates; (3) *the input*: reduce the search of minimal spines from the enormous set of all spines to a much smaller one; this reduction should be achieved by means of *a priori* criteria which do not directly involve the minimality and recognition issues.

Our strategies concerning (1) and (2) are explained in Subsections 1.2 and 1.3. The fact that they are successful for  $n = 9$  is just an experimental evidence, and

we do not add any comment here. Our main contributions concern issue (3). The general idea, explained better in Subsections 1.2 and 1.5, and later expounded in Sections 2 to 5, is that a spine of a manifold often allows to detect many tori embedded in the manifold, and hence to consider the splitting of both the manifold and the spine along these tori. When the original spine is a minimal one, several informations on the pieces resulting from the splitting can be established. This ultimately leads to the notion of the elementary building blocks (called “bricks” below) from which minimal spines are constructed by means of well-understood operations, and to find an input for the algorithm which indeed is dramatically smaller than the set of all spines.

We warn the reader that in Section 2 and 3 many (elementary but) technical definitions are introduced, and that the proofs of the main theorems in Sections 4 and 5 may not be very illuminating by themselves. However the consequences on minimal spines which are eventually deduced in Subsection 5.3 are rather remarkable, and their actual implementation in complexity 9 (anticipated in Subsection 1.6 and explained better in Section 6) is even more remarkable. For instance we can show that 3 bricks only are sufficient to construct a minimal spine of 1145 of the 1156 manifolds of complexity 9. Of the 11 manifolds left, 7 involve 4 other bricks, and the other 4 are themselves bricks, but we know that they will never appear again for higher complexity. Summing up, there are only 7 “interesting” bricks up to complexity 9.

A very useful feature of our decomposition of minimal spines into bricks, originally devised to find a good input for the algorithm, is that it also helps facing the recognition issue. The reason is that to each brick there corresponds a certain ‘block’ (a compact manifold bounded by tori), and a decomposition of a minimal spine into bricks yields a decomposition along tori of the manifold into elementary blocks, so one is only left to analyze the gluings.

The original ideas underlying the algorithm described in this paper, and its actual implementation, are due to the first author. The authors are jointly responsible for the statements and proofs of the purely topological results which show that indeed the algorithm yields the desired result.

## 1 Complexity theory and an overview of the algorithm

### 1.1 Complexity theory

We give here a brief description of complexity theory; for more details see [4]. Throughout this paper we will consider only orientable manifolds and work in the

PL category.

A compact 2-dimensional sub-polyhedron  $P$  of a compact 3-manifold  $M$  is a *spine* of  $M$  if  $M$  collapses onto  $P$ . This can be extended to the closed case, by defining a spine  $P$  of  $M$  a compact 2-dimensional sub-polyhedron  $P \subset M$  such that  $M \setminus P$  is a ball.

A compact polyhedron  $P$  is called *simple* if the link of every point of  $P$  can be embedded in the space given by a circle with three radii. The points having the whole of this space as a link are called *vertices*: they are isolated and therefore finite in number, since every vertex has a neighborhood homeomorphic to the polyhedron shown in Fig. 1-right. This allows to give the following:

**Definition 1.1.** *The complexity  $c(M)$  of a compact 3-manifold  $M$  is equal to  $k$  if it has a simple spine with  $k$  vertices and no simple spines with fewer vertices.*

A simple spine of a closed irreducible orientable 3-manifold  $M$  is *minimal* if it cannot be collapsed onto subpolyhedra and it has  $c(M)$  vertices. The only closed manifolds having complexity zero are  $S^3$ ,  $\mathbb{RP}^3$  and  $L_{3,1}$ , whose minimal spines are respectively a point, the projective plane  $\mathbb{RP}^2$  and the polyhedron obtained by gluing  $D = \{z \in \mathbb{C} : |z| \leq 1\}$  on  $S^1$  along  $\partial D$  via the map  $z \mapsto z^3$ . A closed manifold of higher complexity can have many minimal spines.

A simple polyhedron  $P$  is *quasi-standard* if the link of every point is either a circle, or a circle with a diameter or a circle with three radii (neighborhoods of the point are shown in Fig. 1). Let  $S(P)$  be its singular part, consisting of points of the last two types. We call *1-components* of  $P$  the connected components of  $S(P) \setminus V(P)$ , where  $V(P)$  is the set of vertices of  $P$ , and *regions* of  $P$  the connected components of  $P \setminus S(P)$ . A quasi-standard polyhedron  $P$  is *standard* if the 1-components are open segments (and hence called just *edges*) and the regions are open discs. It is known that a standard spine cannot be the spine of two non-homeomorphic manifolds; moreover Matveev proved the following:

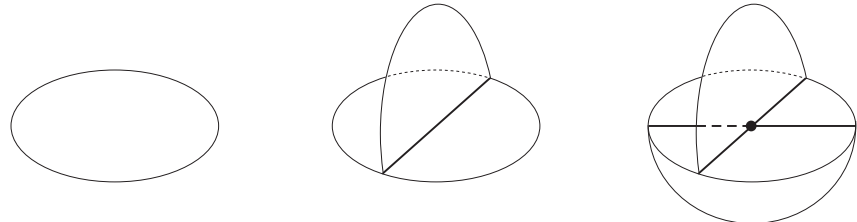


Figure 1: Typical neighborhoods of points in a quasi-standard spine.

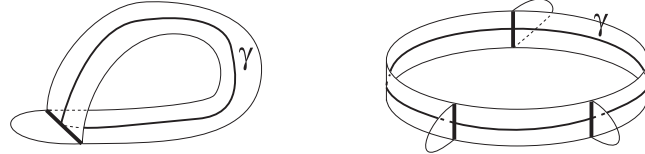


Figure 2: A Möbius strip with a tongue and an annulus with some tongues, all on one side.

**Theorem 1.2.** *Every minimal spine of a closed irreducible orientable manifold  $M$  is standard, except when  $c(M) = 0$ .*

Since there are only finitely many standard polyhedra with  $n$  vertices, this leads to the following property, fundamental for computations: for every  $n \geq 0$ , there is a finite number of closed irreducible 3-manifolds having complexity  $n$ .

## 1.2 Loops and moves

Let  $M$  be a closed orientable manifold and let  $P \subset M$  be a quasi-standard spine of  $M$ . If  $K \subset P$  is any compact subpolyhedron, we will always denote by  $\mathcal{R}_P(K)$  and  $\mathcal{R}_M(K)$  two regular neighborhoods of  $K$ , respectively in  $P$  and  $M$ , such that  $\mathcal{R}_P(K) = \mathcal{R}_M(K) \cap P$ . In most occasions we will consider  $\mathcal{R}_P(K)$  only, and we will shortly denote it by  $\mathcal{R}(K)$ .

A *loop*  $\gamma \subset P$  is a subpolyhedron homeomorphic to  $S^1$  which intersects  $S(P)$  transversely (in particular  $\gamma \cap V(P) = \emptyset$ ). The *length*  $l(\gamma)$  of  $\gamma$  is the number of its intersections with the edges of  $P$ . We say that  $\gamma$  *bounds an external disc* if there exists a closed disc  $D \subset M$  with  $\partial D = \gamma$  and  $D \cap P = \gamma$ . The polyhedron  $\mathcal{R}(\gamma)$  is a *strip* (an annulus or a Möbius band) with  $l(\gamma)$  *tongues* (examples are in Fig. 2). The following remark will be useful:

**Remark 1.3.** A loop  $\gamma$  bounds an external disc if and only if  $\mathcal{R}(\gamma)$  is an annulus having all the tongues on the same side, as in Fig. 2-right. (Note that  $A$  is transversely orientable because  $M$  and  $A$  are orientable.)

Suppose  $\gamma$  bounds an external disc  $D$ . A *disc-replacement move* consists of adding  $D$  to  $P$ , thus getting a spine  $P'$  of  $M$  with two balls  $B', B''$  removed, and then removing a region of  $P'$  homeomorphic to a disc which separates  $B'$  from  $B''$ , yielding another spine of  $M$ .

If  $P$  is standard, then the manifold  $M$  and the way  $P$  sits in  $M$  are well-determined up to homeomorphism, so a disc-replacement move is defined on the abstract  $P$  only, without specifying  $M$ . On the contrary, when  $P$  is quasi-standard,

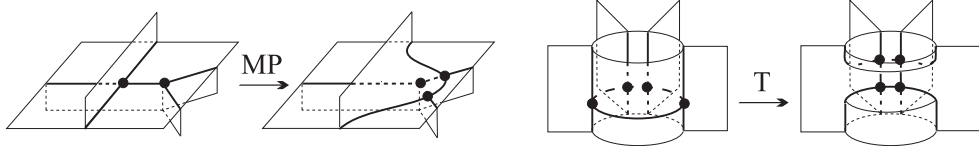


Figure 3: The Matveev-Piergallini move and the T-move.

it is necessary to specify the embedding  $P \hookrightarrow M$  to know which discs of  $P'$  separate  $B'$  from  $B''$ .

Two particular disc-replacement moves are shown in Fig. 3. The first one is the well-known Matveev-Piergallini move, which we denote by MP, in which we add a disc  $D$  with  $l(\partial D) = 4$  and we remove a region with 3 vertices. This move is important because any two standard spines of the same manifold  $M$  are known to be related by combinations of moves  $MP^{\pm 1}$ , except when  $c(M) \leq 1$  (see [1] for references). The second move is one introduced by Matveev in [4], that we denote by T, performed by adding a disc  $D$  with  $l(\partial D) = 4$  and then removing a region with 4 vertices. We note that MP and T are well-defined even if  $P$  is not standard.

A loop is *fake* if it is contained in the link of a point of  $P$ . The following non-minimality criterion is crucial for our algorithm. It will be proved in Subsection 2.2.

**Theorem 1.4.** *Let  $P$  be a standard spine of a closed manifold. Assume that  $P$  contains a non-fake loop which bounds an external disc and has length at most 3. Then  $P$  is not minimal.*

### 1.3 The main algorithm

As already mentioned, the most general problem of complexity theory is to list without repetitions the set  $\mathcal{M}_n$  of all (closed, oriented, irreducible, 3-dimensional) manifolds of a given complexity  $n$ . A general strategy would be to consider the set  $\mathcal{A}_n$  of all standard spines with  $n$  vertices of closed orientable manifolds, test each element of  $\mathcal{A}_n$  for minimality, and recognize the manifolds represented by the minimal elements of  $\mathcal{A}_n$ , so to eliminate duplicates. One practical and two theoretical difficulties arise in connection with this strategy:

1. The test for minimality tacitly involves considering *all* spines related by MP-moves to a given one, so it cannot be carried out in finite time;
2. No general algorithm exists for recognizing a manifold or for checking whether two manifolds are homeomorphic.

3. The whole of  $\mathcal{A}_n$  is an enormous input for an algorithm, even for comparatively small  $n$ ;

The problem of finding a good input for the algorithm will be solved below in Subsection 1.5, using our main achievements about complexity. For the time being, we define a subset  $\mathcal{I}$  of  $\mathcal{A}_n$  to be *complete* if it contains at least one minimal spine of each element of  $\mathcal{M}_n$ , and we assume a complete  $\mathcal{I} \subset \mathcal{A}_n$  to be given. In the rest of this subsection we address the two other problems and give a more precise account of how the algorithm works.

Two ideas underlie the implementation of the minimality test. First, Theorem 1.4 is used to rapidly recognize spines which are not minimal. Second, a restricted set of moves is employed instead of the set of all MP moves. Such a set does not guarantee *a priori* that all non-minimal spines are discarded, but we can experimentally show that it does when  $n = 9$ . Before describing the specific set of moves we have used, we give a definition and provide a general framework for the algorithm. Recall that a complete  $\mathcal{I} \subset \mathcal{A}_n$  is fixed. A set  $\mathcal{S}$  of moves is said to be *admissible* if it has these properties:

1. Every move in  $\mathcal{S}$  transforms a spine  $P \in \mathcal{A}_n$  into a spine  $P' \in \mathcal{A}_n$  of the same manifold;
2. For all  $P \in \mathcal{A}_n$ , it is possible to construct in a finite time the set  $\mathcal{S}(P) \subset \mathcal{A}_n$  of all spines obtained from  $P$  via combinations of moves in  $\mathcal{S}$  ;
3.  $P' \in \mathcal{S}(P)$  if and only if  $P \in \mathcal{S}(P')$  for all  $P, P' \in \mathcal{A}_n$ .

Given  $\mathcal{I}$  (the input) and  $\mathcal{S}$  (the set of moves), the algorithm now works as follows:

- First, it determines which elements of  $\mathcal{I}$  are related to each other through combinations of moves in  $\mathcal{S}$ , and it chooses an arbitrary representative in each class of elements  $\mathcal{S}$ -related to each other;
- Second, it discards from this set of representatives all elements  $\mathcal{S}$ -related to spines to which the non-minimality criterion of Theorem 1.4 applies (note that also spines outside  $\mathcal{I}$  are considered here).

We denote by  $\mathcal{O}(\mathcal{I}, \mathcal{S})$  the output of this algorithm (the choice of representatives is arbitrary, but this will not be relevant). Note that there could be in  $\mathcal{O}(\mathcal{I}, \mathcal{S})$  some non-minimal spines, but if  $\mathcal{I}$  is complete then every element of  $\mathcal{M}_n$  has at least one minimal spine in  $\mathcal{O}(\mathcal{I}, \mathcal{S})$ . We call the pair  $(\mathcal{I}, \mathcal{S})$  an *efficient* one if all spines of  $\mathcal{O}(\mathcal{I}, \mathcal{S})$  are minimal and every element of  $\mathcal{M}_n$  has precisely one spine in  $\mathcal{O}(\mathcal{I}, \mathcal{S})$ . In other words,  $(\mathcal{I}, \mathcal{S})$  is efficient if  $\mathcal{O}(\mathcal{I}, \mathcal{S})$  is a set of spines for  $\mathcal{M}_n$ .

Supposing  $\mathcal{I}$  to be complete, we can test if the pair  $(\mathcal{I}, \mathcal{S})$  is efficient provided that we have already classified  $\mathcal{M}_{<n}$ , and that we are able to recognize manifolds. We simply need to check that the manifolds corresponding to the spines in  $\mathcal{O}(\mathcal{I}, \mathcal{S})$  do not belong to  $\mathcal{M}_{<n}$  and are pairwise distinct. The recognition of manifolds can be done by hand in a reasonable amount of time, finding for each  $n$  new and appropriate techniques, provided  $\mathcal{O}(\mathcal{I}, \mathcal{S})$  is not too big.

As a matter of fact, with the choice of  $\mathcal{I}$  described below, each element of  $\mathcal{I}$ , and hence of  $\mathcal{O}(\mathcal{I}, \mathcal{S})$ , comes with a certain splitting which yields a splitting along tori of the corresponding manifold. The components of this splitting are well-understood and easy, so the recognition problem essentially reduces to writing down certain gluing matrices and checking whether certain Seifert fibrations extend or not. For  $n \leq 9$  this leads for almost all manifolds to an explicit structure of Seifert fibered space, and the tables from [2] are then used for comparison for the other manifolds.

**Choice of moves** The general framework described above for the algorithm was employed, with minor changes, also by Matveev [6]. Besides the choice of the input  $\mathcal{I}$ , which will be discussed below, our approach differs from Matveev's also for the set  $\mathcal{S}$  of moves. Before describing more precisely his and our moves, we note that it would be very interesting to know a priori a class  $\{\mathcal{S}_n : n \in \mathbb{N}\}$  of admissible sets of moves such that  $(\mathcal{A}_n, \mathcal{S}_n)$  is efficient for all  $n$ , because it would give a theoretical algorithm for classifying all closed irreducible 3-manifolds (note that an algorithm which checks irreducibility is known to exist). Matveev has a candidate for such a class, and we have a different one, but in both cases efficiency is only checked for bounded  $n$  and conjectured in general.

Let  $\mathcal{S}_n^{\text{MP}}$  be the set of all combinations of moves MP and  $\text{MP}^{-1}$  that transform a spine of  $\mathcal{A}_n$  into another spine of  $\mathcal{A}_n$ . The pair  $(\mathcal{A}_n, \mathcal{S}_n^{\text{MP}})$  would certainly be efficient, but of course  $\mathcal{S}_n^{\text{MP}}$  is not admissible, because  $\mathcal{S}_n^{\text{MP}}(P)$  cannot be constructed in finite time. The admissible set  $\mathcal{S}_n^{\text{DR}}$  used by Matveev [6] consists of all disc replacement moves with loops of length at most 4 that transform a spine of  $\mathcal{A}_n$  into another spine of  $\mathcal{A}_n$ . The efficiency of  $(\mathcal{A}_n, \mathcal{S}_n^{\text{DR}})$  has been positively tested by Matveev for all  $n \leq 8$ .

The admissible set we have used is the set  $\mathcal{S}_n^{T+1}$  of all combinations of moves T, MP and  $\text{MP}^{-1}$  which start from  $\mathcal{A}_n$  and get back to  $\mathcal{A}_n$ , visiting only  $\mathcal{A}_{\leq n+1}$  at all intermediate steps. We have positively tested the efficiency of  $(\mathcal{I}, \mathcal{S}_n^{T+1})$  for all  $n \leq 9$ , where  $\mathcal{I} \subset \mathcal{A}_n$  is the complete set which we will discuss in Subsection 1.5.

#### 1.4 Splitting of a minimal spine into bricks

This subsection summarizes the contributions given by this paper to the theory of complexity. The technical details of the definitions, statements and proofs are rather

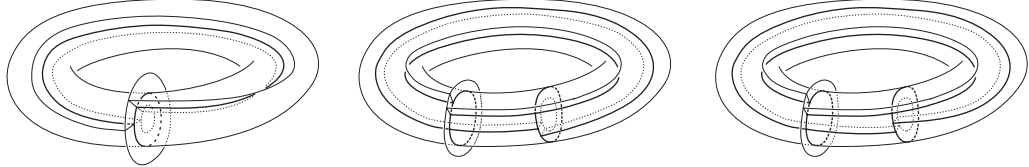


Figure 4: Three types of tori: the first one intersects the spine transversely, the other two are contained in the spine.

complicated and carefully explained in Sections 3 to 5. We only give here a slightly informal account of our main results. We warn the reader that the definitions we will give here will be made more precise later in the paper, and that some results we will state here are only true up to a finite number of well-understood exceptions.

As already mentioned, the splitting of a spine corresponds to a splitting of the associated manifold along tori which are “easily seen” from the spine. Two rather different sorts of tori turn out to be relevant, but quite remarkably both arise from the search of ‘triods’ embedded in the spine. A triod is the graph with two vertices and three edges, none of which is circular, and we require that each edge of the triod is properly embedded in a region of the spine, and that at each vertex of the triod the three germs of edge of the triod lie in the three different germs of region of the spine.

The first type of torus we will consider is one which intersects the spine transversely in one triod, as shown in Fig. 4-left. The second type of torus, which comes in two slightly different variants, is actually contained in the spine itself, and appears as in Fig. 4-center and right. Note that the torus is the union of 4 regions of the spine (2 squares and 2 hexagons in the first variant, 4 pentagons in the second variant), and all 4 these regions are embedded. Moreover a neighborhood of the torus in the spine is bounded by a disjoint union of two triods, so the torus is actually determined by this pair of triods.

Now let a spine be equipped with a finite collection of pairwise disjoint tori, each being of one of the types just described, and remove from the spine a neighborhood of the union of all these tori. The result is a (possibly disconnected) polyhedron which fails to be standard only for having a “boundary”, which consists of a union of triods. To recover standardness, we glue along each boundary triod a copy of the polyhedron shown in Fig. 2-left (there are several ways to do this, we choose one).

The process just described is called a *splitting* of the original spine, and the result is a collection of spines, in which we can actually keep a memory of the process, in the form of the curves  $\gamma$  shown in Fig. 2-left. One can show that the components of

the splitting of a spine are spines of closed manifolds, which are obtained from the original manifold by a splitting along tori followed by a Dehn filling.

There is an obvious counterpart to the operation of ‘splitting’ a spine, which we call ‘assembling’ for obvious reasons. Assembling also comes in two versions, which correspond to the two types of tori along which the splitting is defined. In the first type of assembling, one has two spines each containing a curve as in Fig. 2-left, and the operation consists in removing neighborhoods of the curves and gluing together the two resulting triods. In the second assembling one has two curves on the same spine, and the difference is that now, before gluing the triods, one inserts one of the polyhedra of Fig. 4-center or right.

This discussion suggests the following strategy for listing all manifolds: for each manifold, choose a minimal spine which splits into as many pieces as possible, characterize the spines which cannot be further split, and list their assemblings. A definition and two theorems, all of which will be made more precise below, show that this strategy works.

**Definition 1.5.** *Let  $Q$  be a standard spine of a closed manifold, and let  $\mathcal{L}(Q)$  be the family of all curves in  $Q$  which appear as in Fig. 2-left, up isotopy relative to  $V(Q)$ . We will say that  $Q$  is a brick if it cannot be transformed via moves performed away from  $\mathcal{L}(Q)$  into a spine  $Q'$  such that either  $\#V(Q') < \#V(Q)$ , or  $\#V(Q') = \#V(Q)$  and  $\#\mathcal{L}(Q') > \#\mathcal{L}(Q)$ , or  $\#V(Q') = \#V(Q)$  and  $Q'$  contains a triod not isotopic to the boundary of the neighborhood of any  $\gamma \in \mathcal{L}(Q')$ .*

**Theorem 1.6.** *If  $M$  is a closed, orientable and irreducible 3-manifold, having complexity at most 9 or atoroidal, then  $M$  has at least one minimal spine which splits into bricks.*

The difficult point of this theorem is to show that, once a maximal family of triods in a minimal spine is chosen, the resulting pieces which are not bricks have the special shape of Fig. 4-right. This is *not* true for all minimal spines, and it does require a certain effort to show that one spine with this property exists. The bound 9 is certainly not sharp: we actually conjecture that Theorem 1.6 holds for any closed, orientable and irreducible 3-manifold.

**Theorem 1.7.** *Let  $Q$  be a brick. Then:*

1. *The elements of  $\mathcal{L}(Q)$  are incident to distinct edges of  $Q$ . Each such edge has distinct endpoints and is contained in the closure of precisely two regions. The regions arising by considering the various elements of  $\mathcal{L}(Q)$  are all different from each other.*
2. *No pair of edges disconnects  $S(Q)$ .*

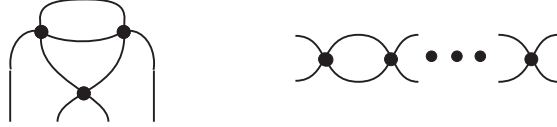


Figure 5: Possible components of the singular set.

3. If a quadruple of edges disconnects  $S(Q)$  then one of the resulting components has one of the shapes shown in Fig. 5.

Concerning the last statement, we note that many more specific informations can actually be established (for instance, we have very precise constraints on the way the regions of  $Q$  can be incident to the graphs of Fig. 5). As a final comment, we note that the definition of *brick* given above is a lot more restrictive than that we will give in Section 3 (for instance, we will not even require standardness). This coarser definition will be useful for the proof of Theorem 1.6, but of course it will make it harder to show Theorem 1.7.

### 1.5 The input for the main algorithm: an algorithm which finds the bricks

Theorem 1.6 implies that if  $\mathcal{B}_{\leq n}$  is the set of all bricks with no more than  $n$  vertices, and  $\langle \mathcal{B}_{\leq n} \rangle$  is the set of all spines obtained by assembling the elements of  $\mathcal{B}_{\leq n}$ , then the subset of  $\langle \mathcal{B}_{\leq n} \rangle$  consisting of spines having  $n$  vertices can be used as an input for the algorithm described in Subsection 1.3. Now  $\mathcal{B}_{\leq n}$  itself is defined in a way which is not directly implementable, because the definition contains a certain notion of minimality and tacitly involves considering arbitrarily long sequences of moves. Nonetheless we have been able to determine  $\mathcal{B}_{\leq 9}$  by choosing a restricted set of moves, which can only give rise to sequences of a bounded length, and by applying an algorithm which works roughly as follows:

1. It lists all the spines satisfying the constraints of Theorem 1.7;
2. It uses the restricted set of moves to eliminate redundancies from the list;
3. It checks that the list thus obtained cannot be further reduced by showing that some manifold of complexity  $\leq 9$  would be missed by a shorter list.

Of course the last step of the algorithm is made necessary by the fact that the set of moves we consider is *a priori* not big enough to guarantee that all redundancies are eliminated. The exact description of the moves we take into account will be

given in Remark 6.1, using technical notions introduced below, but the basic idea is again the same: along sequences of moves we allow only one more vertex than we originally had. As a final remark we note that the set  $\mathcal{B}_{\leq n}$ , which we will introduce in Section 3.3 and call an *n-basis of bricks*, will actually involve an equivalence relation on the set of bricks, due to the fact that what really matters is not the brick itself, but the complement of its preferred set of curves. So  $\mathcal{B}_{\leq n}$  will be a set of representatives, but the algorithm finding it will be exactly as just described.

**Remark 1.8.** We give now an idea of the computer space saved by the use of  $\langle \mathcal{B}_{\leq n} \rangle$  instead of  $\mathcal{A}_n$  as the input for the algorithm. To encode spines combinatorially we have used the *o-graphs* of [1]. Using this encoding, a list (with repetitions) of the elements of  $\mathcal{A}_n$  is obtained as follows. First, find the set  $\mathcal{K}_n$  of all 4-valent graphs with  $n$  vertices, and choose an arbitrary immersion in  $\mathbb{R}^2$  of each  $K \in \mathcal{K}_n$ . Next, recall from [1] that, given  $K \in \mathcal{K}_n$ , an o-graph based on  $K$  is obtained by choosing a color in  $\mathbb{Z}_2$  for each vertex and a color in  $\mathbb{Z}_3$  for each edge. So there are  $2^n 3^{2n}$  o-graphs for each element of  $\mathcal{K}_n$ , and  $\#(\mathcal{K}_n) 2^n 3^{2n}$  in all. Since the same spine is represented by many different o-graphs, the factor  $2^n 3^{2n}$  can often be strongly reduced a priori, by looking at the symmetries of  $K$ , but  $\#(\mathcal{A}_n)$  indeed is big (for instance,  $\#(\mathcal{K}_9) = 8296$  so one can expect  $\#(\mathcal{A}_9)$  to be approximately  $8296 \cdot 18^9 \sim 10^{15}$ . On the contrary,  $\mathcal{B}_{\leq 9}$  consists of 28 spines only, and  $\langle \mathcal{B}_{\leq 9} \rangle$  of less than  $10^5$ .)

**Remark 1.9.** In the same spirit as in the previous remark, we explain now how Theorem 1.7 helps saving space in the search for bricks, by ruling out many elements of  $\mathcal{K}$ . Let  $\mathcal{K}_{\text{brick}}$  consist of graphs which are singular sets of bricks, and let  $\mathcal{H} \subset \mathcal{K}$  consists of the graphs satisfying the constraints of points (2) and (3) of Theorem 1.7. We know that  $\mathcal{K}_{\text{brick}} \subset \mathcal{H} \subset \mathcal{K}$ . The next table lists for  $n \leq 10$  the number of elements of each of these sets, showing that indeed  $\#\mathcal{H}$  is a lot smaller than  $\#\mathcal{K}$ , and not so far from  $\#\mathcal{K}_{\text{brick}}$ . We still have not determined the bricks with 10 vertices, so the last entry of the table is empty.

Vertices	1	2	3	4	5	6	7	8	9	10
$\mathcal{K}$	1	2	4	10	28	97	359	1635	8296	48432
$\mathcal{H}$	1	1	1	2	4	11	27	57	205	1008
$\mathcal{K}_{\text{brick}}$	1	1	1	2	3	1	4	9	13	?

## 1.6 Main results up to complexity 9

According to the results (informally) stated in Subsection 1.4, every manifold without non-separating tori or having complexity at most 9 has a minimal spine which splits into bricks. It is now natural to split the set  $\mathcal{B}$  of bricks as  $\mathcal{B}^0 \sqcup \mathcal{B}^1$ , where  $\mathcal{B}^0$

consists of bricks  $Q$  such that  $\mathcal{L}(Q) = \emptyset$ , which therefore cannot be self-assembled or assembled to other bricks. So we have  $\langle \mathcal{B} \rangle = \mathcal{B}^0 \sqcup \langle \mathcal{B}^1 \rangle$ . The following will be shown in Section 6.

**Proposition 1.10.** *If  $Q \in \mathcal{B}^0$  then  $Q$  is a minimal spine of a closed irreducible manifold, which has no other minimal spine in  $\langle \mathcal{B}^1 \rangle$ .*

According to this fact we can split the set  $\mathcal{M}$  of closed irreducible 3-manifolds as  $\mathcal{M}^0 \sqcup \mathcal{M}^1$ , where manifolds in  $\mathcal{M}^1$  have minimal spines in  $\langle \mathcal{B}^1 \rangle$  and manifolds in  $\mathcal{M}^0$  have some (necessarily minimal) spine in  $\mathcal{B}^0$ .

The algorithm explained in Subsection 1.5 has enabled us to explicitly find  $\mathcal{B}_{\leq 9}^0$ , which consists of 19 spines naturally coming in two families  $C_{i,j}$  and  $E_k$ , and  $\mathcal{B}_{\leq 9}^1$ , which consists of only 9 spines, denoted by  $B_0, \dots, B_8$ . (As mentioned before Remark 1.8,  $\mathcal{B}_{\leq 9}$  is actually a set of representatives of bricks, but we do not insist on this point here.) The 19 manifolds in  $\mathcal{M}^0$  having complexity at most 9, corresponding to the elements of  $\mathcal{B}_{\leq 9}^0$ , are all Seifert fibered over  $S^2$  with 3 exceptional fibers.

The following table summarizes the most relevant information about  $B_0, \dots, B_8$ , with  $v$  and  $L$  denoting respectively the number of vertices and the number of curves in  $\mathcal{L}(B_i)$ . In addition,  $M_i$  is the manifold of which  $B_i$  is a spine. For  $i \leq 4$  and  $i = 8$  the manifold  $M_i$  is a lens space or a Seifert fibered space with 3 exceptional fibers over  $S^2$ , and the usual notation with normalized parameters is used, while it is hyperbolic for  $i = 5, 6, 7$  (here  $H_j$  denotes the closed hyperbolic manifold with  $j$ -th smallest known volume). We also describe the manifold  $N_i$  obtained by drilling the curves of  $\mathcal{L}(B_i)$  out of  $M_i$ . Here we denote by  $D_i$  the disc with  $i$  holes and by  $M_i^k$  the compact manifold with boundary whose interior is the hyperbolic manifold with  $j$ -th smallest volume among the hyperbolic manifolds with  $k$  cusps having complexity  $i$ , as listed in [2]. The complexity of  $N_i$  is shown in the last column. Referring to what stated before Remark 1.8 we note that the  $M_i$ 's depend on the choice of representatives for  $\mathcal{B}_{\leq 9}$ , but the  $N_i$ 's, and all other elements of the table, do not. In particular, the  $M_i$ 's in the table result to be all irreducible and atoroidal, while it is possible to choose representatives so that some  $M_i$  contain incompressible tori for  $i > 0$ . In addition,  $S^2 \times S^1$  is a possible choice for  $M_0$ .

$v$	$B_i$	$L$	$M_i$	$N_i$	$c(N_i)$
0	$B_0$	2	$L_{3,1}$	$D_1 \times S^1$	0
1	$B_1$	2	$L_{4,1}$	$D_1 \times S^1$	0
3	$B_2$	3	$(S^2, (2,1), (2,1), (2,1), (1,-1))$	$D_2 \times S^1$	0
8	$B_3$	1	$(S^2, (2,1), (3,1), (11,2), (1,-1))$	$(D_0, (2,1), (3,1))$	0
8	$B_4$	1	$(S^2, (2,1), (3,2), (3,2), (1,-1))$	$M_2^1$	2
9	$B_5$	1	$H_3$	$M_3^1$	3
9	$B_6$	2	$H_4$	$M_4^2$	4
9	$B_7$	3	$H_1$	$M_6^3$	6
9	$B_8$	3	$(S^2, (2,1), (3,1), (3,2), (1,-1))$	$M_6^3$	6

We next describe our results concerning the number of manifolds in  $\mathcal{M}_c$  for  $c \leq 9$ , summarized by the following table. We have divided the manifolds into three groups, given respectively by the elements of  $\mathcal{M}_{\leq 9}^1$  which may be obtained by assembling  $B_0, \dots, B_8$  but without self-assembling, by those which require a self-assembling, and by those of  $\mathcal{M}^0$ . The three groups have been further split to give a more precise idea of which bricks are needed to generate a manifold: in particular, the vast majority of manifolds (with 11 exceptions out of 1156 manifolds in complexity 9) are generated by  $\{B_0, B_1, B_2\}$ , and only a few manifolds actually require a self-assembling. An important convention in the table is that manifolds already considered in a certain line are not considered again in subsequent lines. (This explains for instance why  $B_7$  and  $B_8$  do not appear; even if some assembling with  $B_0$  indeed are minimal, the corresponding manifolds already appear elsewhere in the table.)

Vertices	1	2	3	4	5	6	7	8	9
$\langle B_0, B_1 \rangle_{\text{non-self}}$	2	3	6	10	20	36	72	136	272
$\langle B_0, B_1, B_2 \rangle_{\text{non-self}}$				2	8	32	97	292	856
$\langle B_0, B_1, B_3 \rangle_{\text{non-self}}$								1	3
$\langle B_0, B_1, B_4 \rangle_{\text{non-self}}$									2
$\langle B_0, B_5 \rangle_{\text{non-self}}$									1
$\langle B_0, B_6 \rangle_{\text{non-self}}$									1
$\langle B_0, B_1 \rangle_{\text{self}}$						5	3	3	7
$\langle B_0, B_1, B_2 \rangle_{\text{self}}$									10
$C_{i,j}$		1	1	2	2	1	2	3	3
$E_v$					1	0	1	1	1
Total	2	4	7	14	31	74	175	436	1156

We add some information which may be of interest, starting with the “easy” manifolds found during the search. The elements of  $\langle B_0, B_1 \rangle_{\text{non-self}}$  are all lens spaces, those of  $\langle B_0, B_1, B_2 \rangle_{\text{non-self}}$  and  $\langle B_0, B_1, B_3 \rangle_{\text{non-self}}$  are graph-manifolds without

non-separating tori, those of  $\langle B_0, B_1 \rangle_{\text{self}}$  are torus bundles over  $S^1$  and those of  $\langle B_0, B_1, B_2 \rangle_{\text{self}}$  are graph-manifolds with graph  $\text{O}\rightarrow$ . As already mentioned, the elements of  $\mathcal{M}^0$  (those which correspond to the  $C_{i,j}$ 's and the  $E_k$ 's) are Seifert fibered over  $S^2$  with 3 exceptional fibers. Since all the manifolds just listed cannot be hyperbolic, we deduce the following:

**Theorem 1.11.** *The only hyperbolic manifolds of complexity 9 are precisely the 4 of least known volume.*

## 2 Surfaces and transverse surfaces in a spine

In the sequel we will need to consider simple polyhedra more general than the quasi-standard ones. A *quasi-standard polyhedron with boundary* is a compact polyhedron  $Q$  in which the link of each point is either as in a quasi-standard polyhedron (Fig. 1), or a closed segment, or the union of 3 closed segments with one common endpoint. The definitions of  $V(Q)$  and  $S(Q)$  still apply. We denote by  $\partial Q$  the set of points of the new types. If the regions given by  $Q \setminus (S(Q) \cup \partial Q)$  are open discs and the 1-components given by  $S(Q) \setminus V(Q)$  are open segments then we call  $Q$  a *standard polyhedron with boundary*.

**Lemma 2.1.** *A standard polyhedron  $Q$ , with or without boundary, is connected if and only if  $S(Q) \cup \partial Q$  is. Moreover, if  $Q$  is standard, connected and not homeomorphic to a disc, the trivalent graph  $\partial Q$  has no component homeomorphic to  $S^1$ .*

*Proof.* Since regions are 2-cells, any path in  $Q$  with endpoints in  $S(Q) \cup \partial Q$  can be homotoped in order to lie in  $S(Q) \cup \partial Q$ .  $\square$

### 2.1 Disconnecting surfaces

For a polyhedron  $X$  and a subpolyhedron  $Y \subset X$  we will denote by  $X_Y$  the closure of  $X \setminus \mathcal{R}(Y)$ , i.e. the result of cutting  $X$  along  $Y$ . We will often apply this definition when  $X$  is a manifold and  $Y$  is a surface, and when  $X$  is a spine and  $Y$  is a graph.

**Proposition 2.2.** *Let  $M$  be a closed orientable manifold and let  $Q \subset M$  be a quasi-standard polyhedron with  $M \setminus Q$  consisting of the disjoint union of two balls  $B', B'' \subset M$ . Then the regions of  $Q$  that separate  $B'$  from  $B''$  form a closed orientable surface  $\Sigma(Q) \subset Q \subset M$  such that  $M_{\Sigma(Q)}$  has two components.*

*Proof.* Let  $e$  be an edge of  $Q$ , and let  $\{f_1, f_2, f_3\}$  be the triple of (possibly not distinct) regions of  $Q$  incident to  $e$ . The number of  $f_i$ 's that separate  $B'$  from  $B''$  is even; it follows that  $\Sigma(Q) \setminus V(Q)$  is a surface, and since  $\Sigma(Q)$  intersects the link of each vertex either nowhere or in a loop, then  $\Sigma(Q)$  is a closed surface. Finally,

$\Sigma(Q)$  disconnects  $M$  because  $B'$  and  $B''$  lie on opposite sides of  $\Sigma(Q)$ . The same argument shows that  $\Sigma(Q)$  is transversely orientable, so it is orientable.  $\square$

**Remark 2.3.** Let  $M$  be a compact orientable 3-manifold, possibly with boundary. A surface  $F$  in a quasi-standard spine  $P \subset M$  contains a graph  $H = F \cap S(P)$  with vertices having valency 3 and 4. If  $F$  is orientable, then we can choose a transverse orientation and give each edge  $e$  of  $H$  a red or black color, depending on whether  $P$  locally lies on the positive or on the negative side of  $F$  near  $e$ . A vertex with valency 3 is adjacent to edges with the same color, and a vertex with valency 4 is adjacent to two opposite red edges and two opposite black ones.

## 2.2 A criterion for non-minimality

The next result, combined with the notion of disc-replacement move, easily implies Theorem 1.4.

**Theorem 2.4.** *Let  $M$  be a closed orientable manifold and let  $P \subset M$  be a quasi-standard spine of  $M$ ; let  $\gamma$  be a non-fake loop bounding an external disc  $D$ , with  $l(\gamma) \leq 3$ . Assume that the regions of  $\Sigma(P \cup D)$  are discs; then there is a region  $f \subset \Sigma(P \cup D)$  of  $P \cup D$  which meets at least  $l(\gamma) + 1$  distinct vertices of  $P \cup D$ .*

*Proof.* We consider the graph  $H = S(P \cup D) \cap \Sigma(P \cup D)$ , that contains  $\partial D$ ; by assumption  $\Sigma(P \cup D) \setminus H$  consists of discs. By Proposition 2.2, the surface  $\Sigma(P \cup D)$  is orientable; we can then choose a transverse orientation and color the edges as explained in Remark 2.3. Suppose by contradiction that each region  $f \subset \Sigma(P \cup D)$  meets at most  $l(\gamma)$  vertices. If  $l(\partial D) = l(\gamma) = 0$  then  $\Sigma(P \cup D)$  is a sphere and  $H = \partial D$  is as in Fig. 6-(1), thus  $\gamma$  is fake.

Suppose  $l(\gamma) \geq 1$ . A vertex in  $\partial D$  has valency 4 if and only if it is adjacent to two distinct edges in  $\partial D$  with distinct colors. If  $l(\gamma) = 1$ , then the only vertex contained in  $\partial D$  would have valency 3, as in Fig. 6-(2). So  $f_1$  would meet at least 2 distinct vertices.

If  $l(\gamma) = 2$ , then the two vertices adjacent to  $\partial D$  have the same valency. Suppose they both have valency 4, as in Fig. 6-(3). Since each  $f_i$  meets at most 2 vertices, then  $H$  is as in Fig. 6-(4), but  $P \cup D$  would be a spine of  $S^3$  with 4 points removed. Suppose both vertices of  $D$  have valency 3: then  $H$  is as in Fig. 6-(5), and  $\gamma$  is fake. Both cases are excluded.

If  $l(\gamma) = 3$ , either all vertices met by  $\partial D$  have valency 3, or two of them have valency 4. Suppose the first case holds. If a region  $f_i$  meets 2 distinct vertices only, then the other two faces adjacent to  $D$  coincide, as in Fig. 6-(6), and meet more than 3 vertices. So each  $f_i$  meets 3 distinct vertices, and  $H$  is the skeleton of the tetrahedron  $\Sigma$  as in Fig. 6-(7); thus  $\gamma$  is fake, which is absurd.

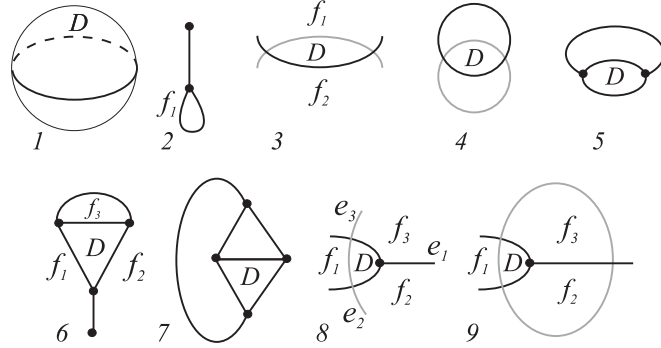


Figure 6: Possible configurations for  $\Sigma(P \cup D)$  in the proof of Theorem 2.4.

Finally, suppose two vertices have valency 4 and one has valency 3 as in Fig. 6-(8); since the region  $f_2$  is incident to at most 3 distinct vertices, then the distinct edges  $e_1, e_2$  have one common endpoint; for the same reason the edges  $e_1, e_3$  have one common endpoint. Then  $H$  is as in Fig. 6-(9); but this is absurd since  $P \cup D$  would be a spine of a manifold with at least 3 boundary components.  $\square$

### 2.3 Simply transverse surfaces

Fundamental properties of complexity theory have been proved in [4] by considering normal surfaces with respect to the handle decomposition of  $M$  given by thickening the cellular structure of  $P$ . In a certain sense, such surfaces are “parallel” to the spine  $P$ . We consider here a different class of surfaces, namely those which are transverse to  $P$ . In contrast with normal surfaces, this class can be defined only when  $M$  is closed.

From now on, we will consider only orientable closed 3-manifolds  $M$  with spines  $P \subset M$  that are quasi-standard in general, and standard only when explicitly mentioned. We denote by  $B$  be the ball  $M \setminus P$ . A closed surface  $F \subset M$  is said to be *simply transverse* to  $P$  if the following requirements are satisfied:

1.  $F$  is transverse to  $P$ ;
2. The intersection of  $F$  with  $B$  consists of a finite number of discs.

The first condition implies that  $Y = P \cap F$  is a finite trivalent graph disjoint from  $V(P)$ , whose vertices lie precisely at the intersection of  $Y$  with the edges of  $P$  (Fig. 7-left). Such a graph is called the *trace* of  $F$ .

Let a trivalent graph  $Y \subset P \setminus V(P)$  be given, in such a way that  $Y \cap S(P)$  consists of all the vertices of  $Y$ , each as in Fig. 7-left. We show that  $Y$  is the trace of

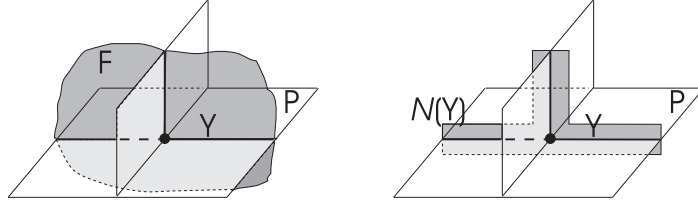


Figure 7: Surface with boundary  $\mathcal{N}(Y)$  constructed from the trivalent graph  $Y$ .

an essentially unique simply transverse surface  $F \subset M$ . First, we can uniquely find a surface  $\mathcal{N}(Y)$  with boundary, transverse to  $P$ , which collapses to  $Y$  (see  $\mathcal{N}(Y)$  near an edge of  $P$  in Fig. 7-right). The boundary of  $\mathcal{N}(Y)$  consists of a finite number of circles that lie on the boundary of a subball  $B'$  of  $B$ . Therefore we can uniquely glue disjoint discs properly embedded in  $B'$  to them, thus getting the desired closed surface  $F$ .

Note that if  $Y$  is the trace of  $F$ , then each component  $D$  of  $F \setminus Y$  is an external disc, and  $\partial D \subset Y$  is a loop if and only if  $D$  is incident to each edge of  $Y$  at most once.

**Remark 2.5.** Let  $Q$  be a standard polyhedron and let  $Y \subset Q$  be a trace without connected components homeomorphic to  $S^1$ . Then  $Q_Y$  is a standard polyhedron with boundary.

**Splitting along simply transverse surfaces** The next statement is in general false for transverse surfaces which are not simply transverse:

**Proposition 2.6.** *Let  $M$  be a closed orientable manifold and let  $P \subset M$  be a quasi-standard spine of  $M$ . Let  $Y \subset P$  be the trace of a simply transverse surface  $F \subset M$ . Then the inclusion  $i : P_Y \hookrightarrow M_F$  induces a bijection  $i_* : \pi_0(P_Y) \rightarrow \pi_0(M_F)$ , and  $F$  is orientable if and only if  $\mathcal{R}_P(Y) \cong Y \times I$ .*

*Proof.* The map  $i_*$  is surjective because each component of  $M_F$  meets  $P$ . Let  $N$  be a connected component of  $M_F$ . We know that  $F \cap B$  consists of discs; therefore  $B \setminus F$  consists of balls  $B^1, \dots, B^n$ , and each path with endpoints in  $P_Y$  and interior in a  $B^i$  can be isotoped in  $B^i$  with fixed endpoints to a path in  $P_Y$ . Therefore any path in  $N$  with endpoints in  $P_Y$  can be homotoped in  $N$  to a path in  $P_Y$ . Thus  $i^{-1}(N)$  is connected.

The second assertion is easy:  $\mathcal{N}(Y) \cong Y \times I \Leftrightarrow F$  has a transverse orientation along  $Y \Leftrightarrow F$  has a global transverse orientation (since  $F \setminus Y$  consists of discs)  $\Leftrightarrow F$  is orientable (since  $M$  is).  $\square$

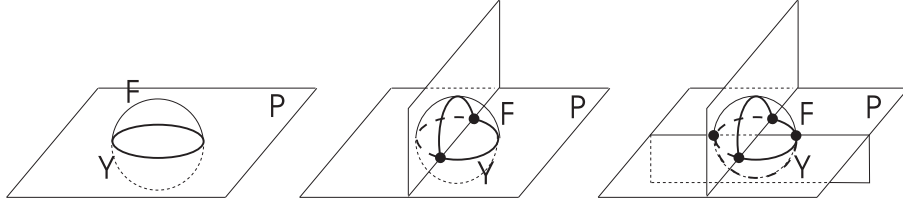


Figure 8: Links of points of  $P$ , and the spheres they are the traces of.

**Links of points and loops** We describe in this paragraph two easy classes of traces. Let  $M$  be a closed manifold and let  $P \subset M$  be a quasi-standard spine of  $M$ . The link of any point  $p$  of  $P$  is the trace of a sphere which bounds a ball (Fig. 8), whose intersection with  $B = M \setminus P$  is given by 2, 3 or 4 discs.

Let  $\gamma \subset P$  be a loop. Recall from Subsection 1.2 that  $\mathcal{R}_M(\gamma)$  is a small regular neighborhood of  $\gamma$  in  $M$ , such that  $\mathcal{R}_M(\gamma) \cap P = \mathcal{R}_P(\gamma)$  is a regular neighborhood of  $\gamma$  in  $P$ , *i.e.* a strip with  $l(\gamma)$  tongues. Then  $\partial\mathcal{R}_P(\gamma) = \partial\mathcal{R}_M(\gamma) \cap P$  is the trace of the torus  $\partial\mathcal{R}_M(\gamma)$  if and only if  $\partial\mathcal{R}_M(\gamma) \setminus \partial\mathcal{R}_P(\gamma)$  consists of discs, namely if and only if there are no annuli in  $\partial\mathcal{R}_M(\gamma) \setminus \partial\mathcal{R}_P(\gamma)$ . By Remark 1.3, there can be such an annulus if and only if  $\gamma$  bounds an external disc.

**$n$ -bridges** Let a 4-valent connected graph  $K$  be given. Let  $\{e_1, \dots, e_{2n}\}$  be distinct edges of  $K$  such that, taking internal points  $p_i \in e_i$ , the polyhedron  $K \setminus \{p_1 \cup \dots \cup p_{2n}\}$  has two connected components  $K_1$  and  $K_2$ , but  $K \cup p_i$  is connected for  $i = 1, \dots, 2n$ . We call  $\{e_1, \dots, e_{2n}\}$  an  $n$ -bridge.

We suppose in this paragraph that  $P$  is a standard spine of a closed manifold  $M$ . Let  $f$  be a region of  $P$  incident to some  $e_i$ . The gluing path of  $\partial f$  to  $S(P)$  can be split into arcs  $s_1, \dots, s_{2k}$ , meeting at points  $q, \dots, q_{2k}$ , where  $s_{2i+1} \subset K_1$  and  $s_{2i} \subset K_2$  for all  $i$ , and each  $q_j$  is glued to one  $p_{\beta(j)}$ . The map  $\beta$  is not necessarily injective, since  $f$  can be multiply incident to an edge  $e_i$ . We can give the vertices  $q_j$  alternating (red and black) colors.

Now take  $k$  pairwise disjoint segments  $\lambda_1, \dots, \lambda_k$ , properly embedded in  $f$ , such that  $\cup_{i=1}^k \partial\lambda_i = \cup_{j=1}^{2k} q_j$ . It is easy to see that the ends of each  $\lambda_i$  necessarily have distinct colors. Note that the  $\lambda_i$ 's are not unique in general. If we do this for each region  $f$  incident to some  $e_i$ , the union of all the chosen segments is a trace  $Y$ . Any trace  $Y$  constructed in this way will be called *orthogonal* to the  $n$ -bridge  $\{e_1, \dots, e_{2n}\}$ .

**Proposition 2.7.** *A trace  $Y$  orthogonal to an  $n$ -bridge is the trace of an orientable surface  $F$ , and  $P_Y$  has two connected components.*

*Proof.* We claim that  $Y$  has a product regular neighborhood in  $P$ : take for each  $i = 1, \dots, 2n$  a vector  $v_i$  at  $p_i$ , tangent to  $e_i$  and directed towards  $K_2$ . Each segment of  $Y$  is a  $\lambda_i$ , properly embedded in a region  $f$  such that  $\partial\lambda_i$  consists of vertices with distinct colors. It follows that the vectors on  $p_i$  extend to a non-vanishing field along  $\lambda_i$  tangent to  $f$ . The existence of such a field on  $Y$  easily implies our claim, and Proposition 2.6 then implies that  $Y$  is the trace of an orientable surface  $F$ .

What already shown implies that  $\partial P_Y$  consists of two disjoint graphs  $Y_1$  and  $Y_2$ , both homeomorphic to  $Y$ . Moreover  $S(P_Y) \cup \partial P_Y$  has two connected components homeomorphic to  $K_1 \cup Y_1$  and  $K_2 \cup Y_2$  (each  $K_i \cup Y_i$  is connected because  $K_i$  is). Adding this to the fact that  $P_Y$  is standard (by Remark 2.5), we deduce that  $P_Y$  has two components.  $\square$

**Triods** Recall that a *triod* is the graph with two vertices and three edges, all joining one vertex to the other one.

**Definition 2.8.** Let  $M$  be a closed manifold and let  $P$  be a quasi-standard spine of  $M$ . We call a triod  $\tau \subset P$  a *toric triod* if the surface having trace  $\tau$  is a torus. We will say that  $\tau$  is a *loop-like* toric triod if  $\tau = \partial \mathcal{R}_P(\gamma)$  for some length-1 loop  $\gamma \subset P$ .

**Remark 2.9.** Let a trace  $\tau \subset P \subset M$  be a triod. In order for  $\tau$  to be toric, since a torus in  $M$  is transversely orientable, we certainly must have that  $\mathcal{R}_P(\tau) \cong \tau \times [-1, 1]$ . In particular  $\mathcal{R}_P(\tau)$  consists of three long rectangles  $R_1, R_2, R_3$  glued along their short edges, and the union of any two of them is an annulus. We concentrate then on the annulus  $A = R_1 \cup R_2$ , and we choose a transverse orientation for  $A$  in  $M$ . Now  $R_3$  is incident to  $A$  along its two short edges, and it locally lies on the positive or on the negative side of  $A$  near either of these edges. If  $R_3$  lies on the positive side near both, as in Fig. 9-left, then  $\tau$  is the trace of a sphere (with the above symbols,  $\mathcal{N}(\tau)$  is as in Fig. 10-left), and the same holds if  $R_3$  lies on the negative side near both edges. On the contrary, if  $R_3$  meets both sides of  $A$ , as in Fig. 9-right, then  $\mathcal{N}(\tau)$  is as in Fig. 10-right and  $\tau$  is toric. Note in particular that the property of  $\tau$  being toric depends not only on the way  $\tau$  sits in  $P$ , but also on the way  $P$  sits in  $M$ . Of course, when  $P$  is standard, only  $\tau \hookrightarrow P$  matters. Note that in Fig. 9 we are also showing  $\mathcal{R}_P(\tau)$  in an unfolded version which includes the transverse orientation in  $M$  and will be useful below.

By this remark, if  $\tau$  is a toric triod and  $T(\tau)$  is the torus defined by  $\tau$ , then  $T(\tau) \setminus \tau$  consists of precisely one disc  $D(\tau)$ .

**Isotopy** When dealing with loops (traces) on a spine  $P$  we will always consider isotopy in which each level is a loop (a trace) and we term it just *isotopy* for the sake of brevity (in particular such an isotopy does not meet  $V(P)$ ).

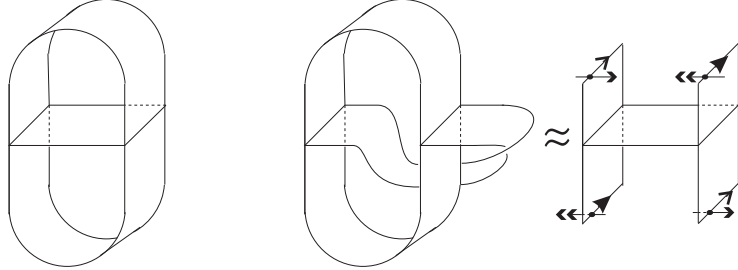


Figure 9: A non-toric and a toric triod.

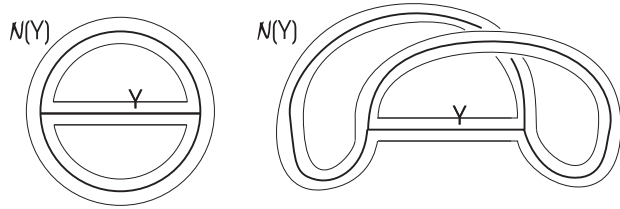


Figure 10: The two possibilities for an orientable  $\mathcal{N}(\gamma)$  when  $\tau$  is a triod.

**Proposition 2.10.** *If  $\gamma$  and  $\gamma'$  are isotopic disjoint loops, then  $\mathcal{R}(\gamma) \cong \mathcal{R}(\gamma')$  is an annulus with some tongues. If  $\tau$  and  $\tau'$  are isotopic disjoint traces, then they both are traces of orientable surfaces and there is a standard sub-polyhedron  $W \subset P$  homeomorphic to  $\tau \times I$  with  $\partial W = \tau \cup \tau'$ .*

*Proof.* The first assertion is due to the following fact: a loop contained in a Möbius strip and isotopic to the strip core must intersect this core. For the same reason, no Möbius strip is contained in  $\mathcal{R}(\tau) \cong \mathcal{R}(\tau')$ . Then we have  $\mathcal{R}(\tau) \cong \tau \times I$  and  $\tau, \tau'$  are both traces of orientable surfaces by Proposition 2.6. The rest of the second assertion easily follows.  $\square$

## 2.4 Co-disconnecting surfaces

The material of this subsection will be useful for proving Theorem 4.2 and in Section 5. Let  $M$  be a closed manifold and let  $P \subset M$  be a quasi-standard spine of  $M$ ; let  $Y \subset P$  be the trace of a surface  $F \subset M$ . Let  $D$  be a component of  $F \setminus Y$ ; the graph  $\partial D \subset Y$  is the union of two graphs  $\partial_1 D, \partial_2 D$ , where  $\partial_i D$  is the closure of the union of the edges of  $Y$  adjacent  $i$  times to  $D$ . It is easy to see that  $\partial_1 D$  is homeomorphic to a disjoint union of circles. Moreover  $\partial_1 D \cap \partial_2 D$  consists of a finite

number of vertices of  $Y$ .

The polyhedron  $P' = P \cup D$  is a spine of  $M$  with two balls  $B', B''$  removed. Note that  $P'$  is quasi-standard  $\Leftrightarrow \partial D$  is a loop  $\Leftrightarrow \partial_2 D = \emptyset$ . Since  $P'$  may not be quasi-standard, we redefine its singular set  $S(P')$  and regions respectively as  $S(P) \cup \partial D$  and as the components of  $P' \setminus S(P')$ . The closure of the union of the regions of  $P'$  that separate  $B'$  from  $B''$  is a subpolyhedron  $\Sigma(P') \subset P'$ . We know by Proposition 2.2 that if  $\partial D$  is a loop then  $\Sigma(P')$  is a closed surface. This is not true in general if  $\partial D$  is not a loop. Putting  $\Sigma_D = \Sigma(P') \setminus D \subset P$ , we have however the following:

**Proposition 2.11.** *The polyhedron  $\Sigma_D \subset P$  is a surface with boundary  $\partial \Sigma_D = \partial_1 D$ . If  $F$  is orientable then  $\Sigma_D \cap \partial_2 D = \partial_1 D \cap \partial_2 D$ ; moreover  $\Sigma(P') \subset M$  is an orientable surface and  $M_{\Sigma(P')}$  has two connected components.*

*Proof.* Let  $s \subset P'$  be a segment, contained in an edge of  $P$ , with  $s \cap \partial D = \emptyset$ ; let  $(f_1, f_2, f_3)$  the triple of (possibly not distinct) regions of  $P'$  incident to  $s$ . The number of  $f_i$ 's that separate  $B'$  from  $B''$  is even. It follows that  $\Sigma_D$  is a surface, possibly with boundary contained in  $\partial D$ .

Let us consider a connected segment  $s \subset \partial D$  with  $s \cap S(P) = \emptyset$ . If  $s \subset \partial_1 D$ , then 3 faces  $(f_1, f_2, D)$  are incident to  $s$ , two of them contained in  $\Sigma(P')$ . Therefore only one  $f_i$  is contained in  $\Sigma_D$ , thus  $\partial_1 D \subset \partial \Sigma_D$ . If  $s \subset \partial_2 D$ , then 4 faces  $(f_1, f_2, D, D)$  are incident to  $s$ , and 2 or 4 of them are contained in  $\Sigma(P')$ . Therefore either both  $f_1$  and  $f_2$  are contained in  $\Sigma_D$ , or none of them is. In both cases  $s \not\subset \partial \Sigma_D$ , and the first assertion is proved. If both  $f_i$ 's are contained in  $\Sigma(P')$ , then  $\overline{D} \subset F$  contains a Möbius strip; so if  $F$  is orientable we have  $\Sigma_D \cap \partial_2 D \subset \partial_1 D \cap \partial_2 D$ , the opposite inclusion being obvious. This shows the second assertion, and the last two follow by the same argument as used in the proof of Proposition 2.2.  $\square$

We say that the surface  $\Sigma_D$  is the *co-disconnecting surface* of the external disc  $D$ ; it depends on  $\partial D$  only, and not on  $Y$ .

**Remark 2.12.** Let a toric triod  $\tau \subset P$  be given. Since  $\partial_1 D(\tau) = \emptyset$ , Proposition 2.11 implies that the polyhedron  $\Sigma_{D(\tau)}$  is a closed surface contained in  $P$ , disjoint from  $\tau$ , which we denote by  $\Sigma_\tau$ ; since  $M_{\Sigma_\tau \cup T(\tau)}$  has two components, then  $\Sigma_\tau$  does not disconnect  $M$ , and  $\Sigma_\tau = \emptyset$  if and only if  $T$  disconnects  $M$ .

### 3 Intrinsic definition of bricks and assembling

#### 3.1 Loop-triod-systems

A *loop-triod pre-system* (also called just *pre-system* for short) is a quadruple  $\Gamma = (M, Q, \mathcal{L}, \mathcal{T})$  where:

- $M$  is a closed orientable (not necessarily irreducible) 3-manifold;
- $Q \subset M$  is a quasi-standard spine of  $M$ ;
- $\mathcal{L} = \{\gamma_i\}$  is a finite set of length-1 loops not bounding external discs;
- $\mathcal{T} = \{\tau_j\}$  is a finite set of toric triods;
- the elements in  $\mathcal{L} \cup \mathcal{T}$  are pairwise disjoint.

We recall that if the regions of  $Q$  are discs then  $M$  and the embedding of  $Q$  in  $M$  are unique, so  $M$  may be dropped from the notation. Proposition 2.10 implies that the loops in  $\mathcal{L}$  are pairwise non-isotopic.

A *system* is a pre-system  $\Gamma = (M, Q, \mathcal{L}, \mathcal{T})$  in which the triods in  $\mathcal{T}$  pairwise non-isotopic, and no such triod is isotopic to a  $\partial\mathcal{R}(\gamma_i)$  for  $\gamma_i \in \mathcal{L}$  (in particular the triods in  $\mathcal{T}$  are non-loop-like). Given a pre-system  $\Gamma = (M, Q, \mathcal{L}, \mathcal{T})$ , we define the polyhedron with boundary  $P_\Gamma = \text{Cl}(Q \setminus \mathcal{R}(\mathcal{L} \cup \mathcal{T}))$ . (Here and in the sequel  $\text{Cl}(S)$  is used as an alternative to  $\overline{S}$  to denote the closure of a set  $S$ .)

Two particular systems are given by  $\Theta_0 = (L_{3,1}, B_0, \{\gamma_1, \gamma_2\}, \emptyset)$  and  $\Theta'_0 = (S^2 \times S^1, B'_0, \{\gamma_1, \gamma_2\}, \emptyset)$ , where  $B_0$  is the minimal spine of  $L_{3,1}$  described in Section 1 and  $B'_0$  is a Klein bottle with a disc glued along a meridian. Both spines can be obtained by appropriately identifying the boundaries of two copies of the Möbius strip with one tongue, shown in Fig. 2-left. The loops  $\gamma_1, \gamma_2$  are then the cores the Möbius strips, and they correspond in the manifold to the cores of the solid tori giving the genus 1 Heegaard splitting.

**Remark 3.1.** A pre-system  $\Gamma \neq \Theta_0, \Theta'_0$  is a system if and only if no component of  $P_\Gamma$  is homeomorphic to  $\tau \times I$ , where  $\tau$  is a triod.

Let  $\Gamma = (M, Q, \mathcal{L}, \mathcal{T})$  be a system. For  $\gamma_i \in \mathcal{L}$  and  $\tau_j \in \mathcal{T}$  we choose the neighborhoods  $\mathcal{R}_M(\gamma_i)$  and the tori  $T(\tau_j)$  so that all the tori  $\{\partial\mathcal{R}_M(\gamma_i), T(\tau_j)\}$  are pairwise disjoint in  $M$ . Then  $\Gamma$  induces a splitting of  $M$  along this set of tori into some blocks  $N_1, \dots, N_l$ . We denote by  $G_\Gamma$  the graph which represents the gluing scheme of the splitting: each vertex of  $G_\Gamma$  represents a block  $N_k$ , and each edge represents a torus in  $\{\partial\mathcal{R}_M(\gamma_i), T(\tau_j)\}$ . We paint in white the vertices representing the blocks  $\mathcal{R}_M(\gamma_i)$ , and in black the other ones. So white vertices have valency 1.

The graphs  $G_{\Theta_0}$  and  $G_{\Theta'_0}$  of the systems defined above would consist of two white vertices (representing  $\mathcal{R}_M(\gamma_1)$  and  $\mathcal{R}_M(\gamma_2)$ ) both joined by one edge only to a black vertex. Since  $B_0, B'_0 = \mathcal{R}_P(\gamma_1) \cup \mathcal{R}_P(\gamma_2)$ , we make an exception to the general rule and stipulate that  $G_{\Theta_0}$  and  $G_{\Theta'_0}$  consist of two white vertices joined by an edge.

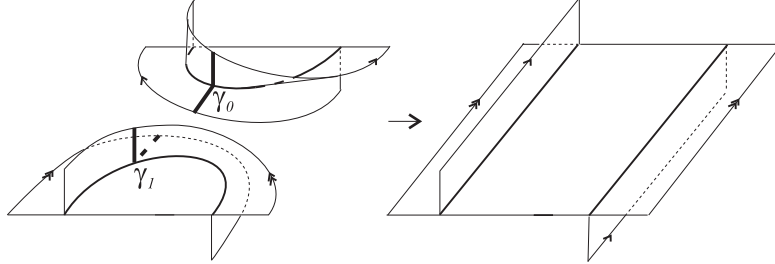


Figure 11: Assembling of two spines. Arcs with equal label are identified.

### 3.2 Assembling

For  $i = 0, 1$  let  $\Gamma_i = (M_i, Q_i, \mathcal{L}_i, \mathcal{T}_i)$  be a system, and pick  $\gamma_i \in \mathcal{L}_i$ . Setting  $P_i = \text{Cl}(Q_i \setminus \mathcal{R}(\gamma_i))$ , we have that  $\partial P_i$  is a triod. We choose now one of the 12 non-isotopic homeomorphisms  $\psi : \partial P_0 \rightarrow \partial P_1$  and consider the polyhedron  $Q = P_0 \cup_{\psi} P_1$  (see a description in Fig. 11). The next result shows that at the level of manifolds the operation just described corresponds to drilling neighborhoods of  $\gamma_0, \gamma_1$  and gluing the drilled manifolds along their toric boundaries.

**Proposition 3.2.** *Put  $N_i = \text{Cl}(M_i \setminus \mathcal{R}_{M_i}(\gamma_i))$ ; then  $Q = P_0 \cup_{\psi} P_1$  is a spine of  $M = N_0 \cup_{\tilde{\psi}} N_1$ , where  $\tilde{\psi} : \partial N_0 \rightarrow \partial N_1$  is a homeomorphism determined by  $\psi$ .*

*Proof.* For  $i = 0, 1$ , the triod  $\partial P_i \subset Q_i$  is the trace of the torus  $\partial N_i \subset M_i$ . The disc  $\partial N_i \setminus \partial P_i$  divides the ball  $M_i \setminus Q_i$  into two open balls  $B_i^0, B_i^1$ ; we can suppose  $B_i^0 \subset N_i$ , for  $i = 0, 1$ . There is a unique way (up to isotopy) to extend the homeomorphism  $\psi : \partial P_0 \rightarrow \partial P_1$  to a homeomorphism  $\tilde{\psi} : \partial N_0 \rightarrow \partial N_1$ . Therefore we can consider  $Q$  as embedded in  $M = N_0 \cup_{\tilde{\psi}} N_1$ . Since  $M \setminus Q = (N_0 \setminus P_0) \cup_{\tilde{\psi}|_{\partial N_0 \setminus \partial P_0}} (N_1 \setminus P_1) = B_0^0 \cup_{\tilde{\psi}|_{\partial N_0 \setminus \partial P_0}} B_1^0$  is a ball, then  $Q$  is a spine of  $M$ .  $\square$

Let  $\tau_{01} \subset Q$  be the triod given by  $\partial P_0$  (or  $\partial P_1$ ), so  $\tau_{01}$  is the trace of the torus  $T(\tau_{01}) \subset M$  given by  $\partial N_0$  or  $\partial N_1$ . Every loop  $\gamma \in (\mathcal{L}_0 \setminus \{\gamma_0\}) \cup (\mathcal{L}_1 \setminus \{\gamma_1\})$  induces a loop in  $Q$  which we keep denoting by  $\gamma$  for simplicity, and every toric triod  $\tau \in \mathcal{T}_0 \cup \mathcal{T}_1$  induces a toric triod in  $Q$ , again denoted by  $\tau$ . We construct the pre-system

$$\Gamma = (M, Q, \mathcal{L}_0 \cup \mathcal{L}_1 \setminus \{\gamma_0, \gamma_1\}, \mathcal{T}_0 \cup \mathcal{T}_1 \cup \{\tau_{01}\}).$$

We have  $P_{\Gamma} \cong P_{\Gamma_0} \sqcup P_{\Gamma_1}$ . Then it follows from Remark 3.1 that  $\Gamma$  is a system, except when  $\Gamma_i = \Theta_0$  or  $\Gamma_i = \Theta'_0$  for  $i \in \{0, 1\}$ . If this holds (suppose  $i = 1$ ), we eliminate  $\tau_{01}$  from  $\Gamma$ , so that  $P_{\Gamma} = P_{\Gamma_0}$  and  $\Gamma$  is a system by Remark 3.1: the spine  $Q$  is obtained from  $Q_0$  just by cutting along the triod  $\partial \mathcal{R}(\gamma_0)$  and gluing back the

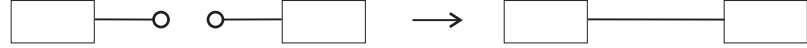


Figure 12: An assembling at the level of graphs.

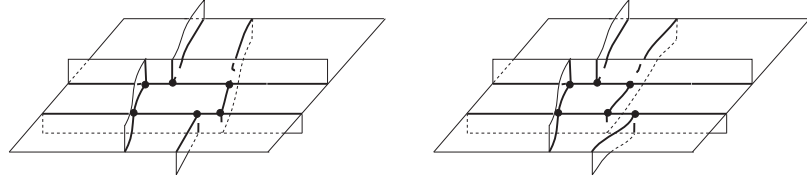


Figure 13: The polyhedra  $\tilde{X}$  and  $\tilde{X}'$ .

two pieces with one of the 12 possible homeomorphisms (but at most 3 of them yield pairwise non-homeomorphic polyhedra).

Both in the general case where  $\{\Gamma_0, \Gamma_1\} \cap \{\Theta_0, \Theta'_0\}$  is empty, and in the special case where it is non-empty, we say that  $\Gamma$  is obtained by *assembling*  $\Gamma_0$  and  $\Gamma_1$  along the loops  $\gamma_0$  and  $\gamma_1$ . The system  $\Gamma$  depends upon the chosen homeomorphism  $\psi$ . The graph  $G_\Gamma$  can be recovered from  $G_{\Gamma_0} \cup G_{\Gamma_1}$  as shown in Fig. 12. Note that this fact crucially depends on our conventions on systems based on  $\Theta_0, \Theta'_0$ .

**Self-assembling** Let a system  $\Gamma = (M, Q, \mathcal{L}, \mathcal{T})$  be given, and let  $\gamma_0, \gamma_1 \in \mathcal{L}$  be distinct loops. Setting  $P = \text{Cl}(Q \setminus \mathcal{R}(\gamma_0 \cup \gamma_1))$ , we have that  $\partial P$  is the union of two triods. Let  $\tilde{X}$  be the polyhedron with boundary shown in Fig. 13-left and obtained from the horizontal square  $[0, 1] \times [0, 1] \times \{0\} \subset \mathbb{R}^3$  by adding vertical (non-straight) strips both above and below the square. Consider the polyhedron  $X$  obtained from  $\tilde{X}$  under the identifications  $(0, y, t) \sim (1, y, t)$  and  $(x, 0, t) \sim (x, 1, t)$ ; let  $X'$  be the polyhedron obtained similarly from the polyhedron  $\tilde{X}'$  shown in Fig. 13-right. Note that because of these identifications  $X$  and  $X'$  are both standard polyhedra with boundary that contain a torus and have a total of 10 regions (4 of which on the torus). The boundary of each consists of two triods. We choose now one of them (say  $X$ ) and one homeomorphism  $\psi : \partial P \rightarrow \partial X$  and consider the polyhedron  $Q' = P \cup_\psi X$  (there are  $2 \cdot 12 \cdot 12$  non-isotopic homeomorphisms, many of them yielding homeomorphic polyhedra).

The next result shows that at the level of manifolds the operation just described corresponds to drilling neighborhoods of  $\gamma_0, \gamma_1$  and identifying the toric boundaries. The statement and proof refer to  $X$ , but they extend *verbatim* to  $X'$ .

**Proposition 3.3.** *Put  $N = \text{Cl}(M \setminus \mathcal{R}_M(\gamma_0 \cup \gamma_1))$ ; then  $Q' = P \cup_\psi X$  is a spine of*

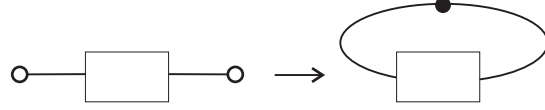


Figure 14: A self-assembling at the level of graphs.

$M' = N \cup_{\tilde{\psi}} (T \times I)$ , where  $T$  is a torus and  $\tilde{\psi} : \partial N \rightarrow T \times \{0, 1\}$  is a homeomorphism determined by  $\psi$ .

*Proof.* Consider the polyhedron  $X$  as embedded in the manifold  $T \times I$  so that  $\partial X = X \cap \partial(T \times I)$  and  $T \times I \setminus X$  consists of two balls  $B', B''$ .

The two triods given by  $\partial P \subset Q$  are traces of the two tori given by  $\partial N \subset M$ . Then  $\partial N \setminus \partial P$  consists of two discs  $D_0, D_1$ , that divide the ball  $M \setminus Q$  into three open balls  $B^0, B^1, B^2$ ; we can suppose  $B^2 \subset N$  and  $B^0, B^1 \subset M \setminus N$ . There is a unique way (up to isotopy) to extend the homeomorphism  $\psi : \partial P \rightarrow \partial X$  to a homeomorphism  $\tilde{\psi} : \partial N \rightarrow \partial(T \times I)$ . Therefore we can consider  $Q'$  as embedded in  $M' = N \cup_{\tilde{\psi}} (T \times I)$ . Since  $M' \setminus Q' = (N \setminus P) \cup_{\tilde{\psi}|_{\partial N \setminus \partial P}} (T \times I \setminus X) = B^2 \cup_{\tilde{\psi}|_{D_0 \cup D_1}} (B' \cup B'')$  is a ball, then  $Q'$  is a spine of  $M'$ .  $\square$

Let  $\tau_0, \tau_1 \subset Q'$  be the triods given by  $\partial P$  (or  $\partial X$ ). They are traces of two parallel tori in  $M'$ , each parallel to the torus  $T$  contained in  $X$  (but  $\tau_0$  and  $\tau_1$  are not isotopic in general). Every loop  $\gamma \in \mathcal{L} \setminus \{\gamma_0, \gamma_1\}$  induces a loop in  $Q'$ , which we keep denoting by  $\gamma$  for simplicity, and every toric triod  $\tau \in \mathcal{T}$  induces a toric triod in  $Q'$ , again denoted by  $\tau$ . We construct the pre-system

$$\Gamma' = (M', Q', \mathcal{L} \setminus \{\gamma_0, \gamma_1\}, \mathcal{T} \cup \{\tau_0, \tau_1\}).$$

We have  $P_{\Gamma'} \cong P_{\Gamma} \sqcup X$ . It follows then from Remark 3.1 that  $\Gamma'$  is a system, except when  $\Gamma = \Theta_0, \Theta'_0$ . If this holds, we eliminate either  $\tau_0$  (or  $\tau_1$ ) from  $\Gamma'$ , so that  $P_{\Gamma'} = X$  and  $\Gamma'$  is a system by Remark 3.1: the spine  $Q'$  is simply obtained from  $X$  by identifying its two boundary components.

Both when  $\Gamma$  is one of  $\Theta_0, \Theta'_0$  and when it is not, we say that  $\Gamma'$  is obtained by *self-assembling*  $\Gamma$  along the loops  $\gamma_0, \gamma_1 \in \mathcal{L}$  via  $X$  (everything said works with  $X'$  too). The system  $\Gamma'$  depends upon the choice between  $X$  and  $X'$  and upon the homeomorphism  $\psi$ . The graph  $G_{\Gamma'}$  can be recovered from  $G_{\Gamma}$  as shown in Fig. 14. This fact crucially depends on our conventions on  $\Theta_0, \Theta'_0$ : when  $\Gamma \in \{\Theta_0, \Theta'_0\}$  then  $G_{\Gamma'}$  is a graph with one black vertex and one edge with coinciding endpoints.

**Remark 3.4.** In a pattern of assemblings and self-assemblings, if a system  $\Theta_0$  or  $\Theta'_0$  appears and is assembled along both its white vertices, then the pattern is equivalent

to one in which such a system is removed, because  $P_{\Theta_0} \cong P_{\Theta'_0}$  is a triod times an interval.

### 3.3 Bricks and bases

**Lemma 3.5.** *Let  $M$  be a closed manifold and let  $Q \subset M$  be a quasi-standard spine of  $M$ . Let  $D$  be an external disc bounded by a loop  $\gamma \subset Q$ , or a component of  $F \setminus Y$  where  $Y \subset Q$  is the trace of a surface  $F$ . Let  $\eta$  be either a toric triod or a length-1 loop not bounding an external disc. If  $\partial D \cap \eta = \emptyset$ , then  $\Sigma_D \cap \eta = \emptyset$ .*

*Proof.* Suppose  $\eta$  is a toric triod. Since  $\eta \cap \partial D = \emptyset$ , then  $T(\eta) \cap \partial D = \emptyset$  and we can suppose that  $T(\eta) \cap D = \emptyset$ . Let  $B', B''$  be the two open balls given by  $M \setminus (Q \cup D)$ . Then  $D(\eta)$  lies in one of them, say  $B'$ , so  $T(\eta) \cap \Sigma_D = \emptyset$ , whence  $\eta \cap \Sigma_D = \emptyset$ .

If  $\eta$  is a loop, the same argument applies to the toric triod  $\partial\mathcal{R}(\eta)$ .  $\square$

**Definition 3.6.** *Let  $\Gamma = (M, Q, \mathcal{L}, \mathcal{T})$  be a system. A compact polyhedron  $K \subset Q$  is said to be free if it is disjoint from all the elements of  $\mathcal{L} \cup \mathcal{T}$ .*

Let  $\Gamma = (M, Q, \mathcal{L}, \mathcal{T})$  be a pre-system and let  $\gamma \subset Q$  be a free loop bounding an external disc  $D$ . We can perform on  $Q$  a disc-replacement move by adding  $D$  and removing a region of  $\Sigma(Q \cup D)$  homeomorphic to a disc, getting a spine  $Q'$ . By Lemma 3.5, each  $\gamma \in \mathcal{L}$  induces a loop in  $Q'$ , which we keep denoting by  $\gamma$  for simplicity, and each  $\tau \in \mathcal{T}$  induces a toric triod in  $Q'$ , again denoted by  $\tau$ . Therefore  $\Gamma' = (M, Q', \mathcal{L}, \mathcal{T})$  is a pre-system. If both  $\Gamma$  and  $\Gamma'$  are systems we say that we have performed a *system-move* that transforms  $\Gamma$  into  $\Gamma'$ . Note that we have  $G_{\Gamma'} = G_{\Gamma}$ : system-moves do not affect the manifold  $M$  and its splitting induced by  $\Gamma$ .

**Bricks** Let a system  $\Gamma = (M, Q, \mathcal{L}, \mathcal{T})$  be given. We denote by  $\mathcal{Y}(\Gamma)$  the (infinite) set of systems (up to isomorphism) obtained from  $\Gamma$  via combinations of system-moves.

**Definition 3.7.** *Let  $\Gamma = (M, Q, \mathcal{L}, \mathcal{T})$  be a system. We call  $\Gamma$  maximal if there is no system  $(M, Q, \mathcal{L}', \mathcal{T}')$  with  $\mathcal{L}' \cup \mathcal{T}' \supsetneq \mathcal{L} \cup \mathcal{T}$ . We call  $\Gamma$  fundamental if it satisfies the following properties:*

1. *For each  $\Gamma' = (M, Q', \mathcal{L}', \mathcal{T}') \in \mathcal{Y}(\Gamma)$  we have  $\#V(Q') \geq \#V(Q)$ ;*
2. *If  $\Gamma' = (M, Q', \mathcal{L}', \mathcal{T}') \in \mathcal{Y}(\Gamma)$  and  $\#V(Q') = \#V(Q)$ , then  $\Gamma'$  is maximal and every length-0 free loop bounding an external disc is fake.*

*We call  $\Gamma$  a brick if it is fundamental and  $\mathcal{T} = \emptyset$ .*

**Remark 3.8.** A system  $\Gamma = (M, Q, \mathcal{L}, \mathcal{T})$  is maximal if and only if every toric triod in  $P_\Gamma$  is isotopic to a boundary component.

**Proposition 3.9.** *A fundamental system  $\Gamma = (M, Q, \mathcal{L}, \mathcal{T})$  is maximal. If  $Q \neq \mathbb{RP}^2$ , then  $P_\Gamma$  is standard.*

*Proof.* Since  $\Gamma \in \mathcal{Y}(\Gamma)$ , then  $\Gamma$  is maximal and  $P_\Gamma$  does not contain non-fake length-0 loops bounding external discs. If  $P_\Gamma$  is not standard, then it contains a non-fake length-0 loop  $\gamma$ . Since  $\gamma$  cannot bound an external disc, then  $\mathcal{R}(\gamma)$  is a Möbius strip whose boundary is a loop that bounds an external disc. Thus  $\partial\mathcal{R}(\gamma)$  is fake, and  $Q = \mathbb{RP}^2$ .  $\square$

**Proposition 3.10.** *An assembling of two systems is fundamental if and only if the original systems are, and a self-assembling of a system is fundamental if and only if the original system is.*

*Proof.* Let  $\Gamma$  be an assembling of  $\Gamma_0$  and  $\Gamma_1$ . Suppose  $\Gamma_0, \Gamma_1$  are fundamental; we prove that  $\Gamma$  is. Every  $\Gamma' \in \mathcal{Y}(\Gamma)$  is obtained from  $\Gamma$  via combinations of system-moves; such a combination projects to a combination of system-moves that transform  $\Gamma_0 \sqcup \Gamma_1$  into  $\Gamma'_0 \sqcup \Gamma'_1$ , with  $\Gamma'_i \in \mathcal{Y}(\Gamma_i)$ , such that  $\Gamma'$  is an assembling of  $\Gamma'_0$  and  $\Gamma'_1$ . Then  $\Gamma'$  must have at least the same number of vertices of  $\Gamma$ , since each  $\Gamma'_i$  has at least the same number of vertices of  $\Gamma_i$ . Suppose  $\Gamma$  and  $\Gamma'$  have the same number of vertices: since  $\Gamma_0$  and  $\Gamma_1$  are fundamental, then  $P_{\Gamma'_0}$  and  $P_{\Gamma'_1}$  do not contain non-fake length-0 loops bounding discs, and toric triods are isotopic to boundary components. The conclusion now follows from the definition and from Remark 3.8, since  $P_{\Gamma'} \cong P_{\Gamma'_0} \sqcup P_{\Gamma'_1}$  (or  $P_{\Gamma'} \cong P_{\Gamma'_i}$  if  $\Gamma'_i \in \{\Theta_0, \Theta'_0\}$  for some  $i$ ).

The other cases are proved with the same method.  $\square$

Two bricks  $\Gamma, \Gamma'$  are said to be *similar* if  $\Gamma$  is obtained by assembling  $\Gamma'$  and some copies of  $\Theta_0$ , *i.e.* if  $P_\Gamma = P_{\Gamma'}$ . In particular,  $\Theta_0$  and  $\Theta'_0$  are similar. We consider the following equivalence relation on the set of all bricks with  $n$  vertices: two bricks  $\Gamma, \Gamma'$  are equivalent if and only if  $\Gamma' \in \mathcal{Y}(\Gamma'')$  for some  $\Gamma''$  similar to  $\Gamma$ . A set  $\mathcal{B}_n$  of representatives is called an *n-basis*. It is easy to prove the following:

**Fact 3.11.** *A 0-basis  $\mathcal{B}_0$  is given by two elements:  $\Theta_0$  and  $(\mathbb{RP}^3, \mathbb{RP}^2, \emptyset, \emptyset)$ .*

## 4 Splitting of a minimal spine into bricks

Let  $\mathcal{B}$  be a set of bricks, which by default we assume to contain  $\Theta_0$ . We denote by  $\langle \mathcal{B} \rangle$  the set of systems obtained by first assembling some elements taken from  $\mathcal{B}$ , with repetitions, and then doing some self-assemblings on the result. As usual, systems are viewed up to isomorphism.

**Remark 4.1.** By Remark 3.4, when considering  $\langle \mathcal{B} \rangle$  for a set  $\mathcal{B}$  of bricks, we only need to first assemble (with repetition) the elements of  $\mathcal{B}$  having positive complexity, *i.e.* those different from  $\Theta_0$ . Then we do some self-assembling on the result, and only then we assemble some  $\Theta_0$ 's. This fact can be of some use in giving *a priori* estimates on the number of elements of  $\langle \mathcal{B} \rangle$  having a certain bound on complexity.

The following is our main result:

**Theorem 4.2.** *Let  $n \geq 1$  and let  $\mathcal{B}_l$  be an  $l$ -basis for all  $0 \leq l \leq n$ . Let  $M$  be a closed irreducible manifold of complexity  $n$ . Assume either that in  $M$  all tori are separating or that  $n \leq 9$ . Then  $M$  has a minimal spine  $P$  which belongs to  $\langle \bigcup_{l=0}^n \mathcal{B}_l \rangle$ .*

*Proof.* The statement of course means that  $M$  has a minimal  $P$  which embeds in a system  $(M, P, \mathcal{L}, \mathcal{T})$  lying in  $\langle \bigcup_{l=0}^n \mathcal{B}_l \rangle$ . Taking into account the equivalence relation used to define the notion of basis of bricks, it is actually sufficient to show that there exists a system  $(M, P, \mathcal{L}, \mathcal{T})$  which splits into bricks, because we can always replace a brick in the splitting with its equivalent in  $\bigcup_{l=0}^n \mathcal{B}_l$ .

Our proof is long and organized in 4 main steps. Most of our assertions actually hold without any assumption on  $M$  other than irreducibility, and we will give general proofs even when the extra assumptions would allow a shorter argument. We will emphasize the points which we can presently show only assuming atoroidality or  $n \leq 9$ .

**Step 1. Existence of a fundamental system.** Consider any system  $(M, P, \mathcal{L}, \mathcal{T})$  where  $P$  is a minimal spine of  $M$ . We show that  $\#(\mathcal{L} \cup \mathcal{T})$  can be bounded in terms of  $n$ , which easily implies, by a maximality argument, that there exists a fundamental system involving a minimal spine of  $M$  (we do not need to check the cellularity condition, because minimal spines are always standard for  $n \geq 1$ .)

We first show that  $\#\mathcal{L} \leq 6n$ . This is because each element  $\gamma$  of  $\mathcal{L}$  is determined by the edge  $e$  of  $P$  it meets and by the two germs of region of  $P$  incident to  $e$  in which  $\gamma$  locally lies near  $\gamma \cap e$ . There are  $2n$  edges and 3 germs of region incident to each edge, and the conclusion follows.

We next show that  $\#\mathcal{T} \leq 18n^2$ . Just as above, a triod is determined by the two edges it meets and by the germs of regions it locally lies in. For any pair of edges there are at most 9 triods, and there are no more than  $2n^2$  pairs of edges.

**Step 2. The co-disconnecting surface of the triods consists of disjoint small tori.** Assume from the first step that  $\Gamma = (M, P, \mathcal{L}, \mathcal{T})$  is a fundamental system with  $P$  minimal spine of  $M$ . Recall that for  $\tau \in \mathcal{T}$  we denote by  $T(\tau)$  the torus whose trace is  $\tau$ , and by  $D(\tau)$  the open disc  $T(\tau) \setminus \tau$ . Let us consider now the co-disconnecting surfaces  $\Sigma_\tau$  of the  $D(\tau)$ 's. Remark 2.12 shows that  $\Sigma_\tau$  is a (possibly disconnected) closed orientable and non-separating surface disjoint from  $T(\tau)$ . Our aim is now to

show that, up to changing the choice of  $\Gamma$ , the various  $\Sigma_\tau$ 's are pairwise disjoint and each (if non-empty) consists of “small tori,” *i.e.* toric components having regular neighbourhood in  $P$  homeomorphic to one of the spaces  $X, X'$  shown in Fig. 13. This will later allow us to conclude that  $(M, P, \mathcal{L}, \mathcal{T})$  indeed splits into bricks.

We will now prove the assertions of Step 2 leaving the main technical point as an independent claim, to be proved below as Step 3. We first choose an arbitrary ordering  $\tau_1, \dots, \tau_k$  for the elements of  $\mathcal{T}$ , and we note that if  $\Gamma'$  is obtained from  $\Gamma$  by a combination of system-moves then there is an induced ordering also on the triods of  $\Gamma'$ .

We now claim the following: *Assume  $h \geq 1$  and  $\Sigma_{\tau_i} \cap \Sigma_{\tau_h} = \emptyset$  for  $i < h$ . Replace  $\Gamma$  by the system  $\Gamma'$  related to  $\Gamma$  via system-moves and having the property that  $\#(V(P') \cap \Sigma_{\tau'_i}) = \#(V(P) \cap \Sigma_{\tau_i})$  for  $i < h$ , whereas  $\#(V(P') \cap \Sigma_{\tau'_h})$  is minimal among all such systems. Then  $\Sigma_{\tau'_h}$  is empty or it consists of small tori.*

Assuming this claim, we show how to conclude Step 2. We first apply the claim with  $h = 1$  (so the hypothesis is automatically true), and we deduce that  $\Sigma_{\tau_1}$  is empty or consists of small tori. In particular,  $\partial\mathcal{R}(\Sigma_{\tau_1})$  consists of triods, which can be chosen to be close enough to  $\Sigma_{\tau_1}$  to be free. Then, by the maximality of  $\Gamma$ , these triods are isotopic either to some  $\tau' \in \mathcal{T}$  or to some  $\partial\mathcal{R}(\gamma)$  for  $\gamma \in \mathcal{L}$ , but the latter is impossible otherwise  $\Sigma_{\tau_1}$  would separate. In particular  $\partial\mathcal{R}(\Sigma_{\tau_1})$  is disjoint from  $\tau_i$  for  $i > 1$ , so  $\partial\mathcal{R}(\Sigma_{\tau_1})$  is disjoint from  $\Sigma_{\tau_i}$  for  $i > 1$  (by Lemma 3.5), and hence  $\Sigma_{\tau_1}$  is also disjoint from  $\Sigma_{\tau_i}$  for  $i > 1$ . We are now in a position to apply the claim again for  $h = 2$ , and the conclusion easily follows by iterating this method.

**Step 3. Proof of the main claim.** For simplicity we denote  $\tau_h$  by  $\tau$ , and we refer to the  $\Sigma_{\tau_i}$ 's for  $i < h$  as “previous surfaces.” If all tori in  $M$  are separating then  $\Sigma_\tau = \emptyset$ , and we have nothing to prove. Otherwise, assume that  $n \leq 9$  and that  $\Sigma_\tau \neq \emptyset$ . Since  $M$  is irreducible and  $\Sigma_\tau$  is non-separating, no component of  $\Sigma_\tau$  can be homeomorphic to  $S^2$ . Note also that  $\Sigma_\tau$  is free by Lemma 3.5, so a disc replacement near  $\Sigma_\tau$  is automatically a system-move. Moreover  $\Sigma_\tau$  is disjoint from the previous surfaces, so such a system-move is one of those taken into account in the statement of the claim for the minimization of  $\#(V(P) \cap \Sigma_\tau)$ .

We concentrate now on a component  $\Sigma$  of  $\Sigma_\tau$ . Choosing a transverse orientation for  $\Sigma$  as in Remark 2.3, we can trace on  $\Sigma$  two trivalent graphs  $Y_+$  and  $Y_-$  which intersect transversely. These graphs represent the way the rest of  $P$  glues to  $\Sigma$ , and the sign  $+$  or  $-$  depends on whether  $P$  locally lies on the positive or on the negative side of  $\Sigma$ . We show now several properties of the triple  $(\Sigma, Y_+, Y_-)$ .

1.  $\Sigma \setminus Y_\pm$  consists of planar surfaces. Given a point  $p$  of  $\Sigma \setminus (Y_+ \cup Y_-)$  there are two points  $p_+, p_-$  of  $\partial\mathcal{R}_M(P)$  closest to  $p$ , with  $p_+$  on the positive side of  $\Sigma$  and  $p_-$  on the negative side. It is not hard to show that the map  $p \mapsto p_+$

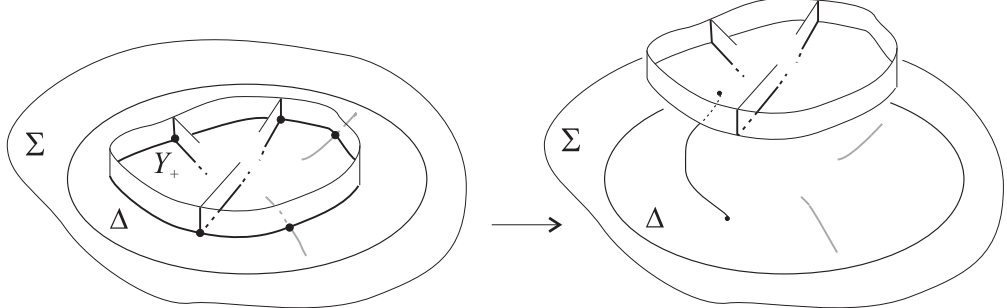


Figure 15: A move which reduces complexity.

extends to a homeomorphism of  $\Sigma \setminus Y_+$  onto an open subset of  $\partial \mathcal{R}_M(P) \cong S^2$ , and similarly for  $Y_-$ .

2. *The components of  $\partial \mathcal{R}(Y_\pm)$  bound discs in  $M$ .* This follows from the same argument just explained.
3.  $\Sigma \setminus (Y_+ \cup Y_-)$  consists of discs. This is because  $\Sigma \subset P$ ,  $Y_+ \cup Y_- = \Sigma \cap S(P)$ , and  $P$  is standard.
4. *If a component of  $\Sigma \setminus \mathcal{R}(Y_\pm)$  is not a disc then its boundary loops are essential in  $\Sigma$ .* We refer to  $Y_+$ . If one of them is not, it is very easy to see that there is a disc  $\Delta$  in  $\Sigma$  such that  $Y_+ \cap \partial \Delta = \emptyset$  but  $Y_+ \cap \Delta \neq \emptyset$ , so in particular  $Y_+ \cap \Delta$  contains vertices of  $P$ . The move suggested in Fig. 15 then contradicts the minimality of  $P$ .
5. *Not all the components of  $\mathcal{R}(Y_\pm)$  are planar.* Again we refer to  $Y_+$ . By contradiction, from points 1 and 2 and the irreducibility of  $M$ , we would readily get that  $\Sigma$  bounds a handlebody, which is absurd.
6. *Every component of  $Y_+$  intersects  $Y_-$ , and conversely.* Otherwise, since  $\Sigma$  is connected, there would exist a component of  $\Sigma \setminus (Y_+ \cup Y_-)$  with disconnected boundary, contradicting point 3.
7.  *$Y_+ \cap Y_-$  contains at least two points.* Assume there is only one point  $v$  (a crossing between  $Y_+$  and  $Y_-$ ). If a region  $f$  of  $\Sigma$  is incident to  $v$ , then it must be multiply incident, because regions contain an even number of quadrivalent vertices (with multiplicity). If two instances of  $f$  are adjacent to each other at  $v$ , we find in the closure of  $f$  a length-1 loop bounding an external disc, which contradicts minimality. If two instances of  $f$  are opposite at  $v$ , then for the

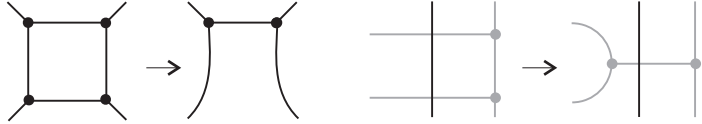


Figure 16:  $T$ -moves on forbidden squares. Different colors are used to distinguish  $Y_+$  and  $Y_-$ .

same reason there is another region  $g$  doubly incident to  $v$ , and  $g \neq f$ . Now in the closure of  $f \cup g$  we can easily find a length-2 loop bounding an external disc which meets edges opposite at  $v$ . By minimality the loop must be fake, so these edges must actually be the same. Orientability of  $\Sigma$  then implies that  $f = g$ : a contradiction.

8. *If a component of  $Y_+$  is a circle then it intersects  $Y_-$  in at least 4 points, and conversely.* This readily follows from minimality, because this circle is precisely the boundary of a region of  $P$  (see Corollary 5.3).
9. *No squares as in Fig. 16 occur in  $(\Sigma, Y_+, Y_-)$ .* This follows from the assumption that the number of vertices in  $Y_+ \cup Y_-$  should be minimal, because otherwise a  $T$ -move allows to reduce this number, as shown in Fig. 16 itself. Note that the  $T$ -move takes place near  $\Sigma$ , so it does not affect the previous surfaces, and the move indeed is one of those considered in the statement of the claim.

We show now how to conclude Step 3, using the fact that  $n \leq 9$ . It follows from point 5 that both  $Y_+$  and  $Y_-$  have vertices. Being trivalent, they have an even number of them, and the total is at most  $9 - 2 = 7$  by point 7. So up to permutation we can assume that  $Y_+$  has 2 vertices. In particular  $\mathcal{R}(Y_+)$  has only one non-planar component, which is homeomorphic to a punctured torus (with a component of  $Y_+$  sitting as a triod in this torus). From point 8 we deduce that  $Y_+$  can have at most one circular component, and is it now easy to deduce from point 1 that  $\Sigma$  indeed is a torus. Point 4 then implies that  $Y_+$  consists of the triod only.

In the rest of our proof we will always depict  $\Sigma$  cut open along  $Y_+$ . So  $\Sigma$  appears as a hexagon, and we denote by  $\Delta$  its interior. Our aim is to show that  $Y_-$  also has 2 vertices and that it appears in one of the two shapes shown in Fig. 17, because these two shapes exactly correspond to the polyhedra  $X$  and  $X'$  of Fig. 13. To show this we first rule out the possibility that  $Y_-$  has 4 vertices, and then carefully analyze the possibilities with 2 vertices.

So, let  $Y_-$  have 4 vertices. We claim that all the components of  $Y_- \cap \Delta$  are trees. If one of them is not then there is a region of  $P$  inside  $\Delta$  and bounded by  $Y_-$ . Then either this region has  $\leq 3$  vertices, which contradicts minimality of  $P$ , or it has the

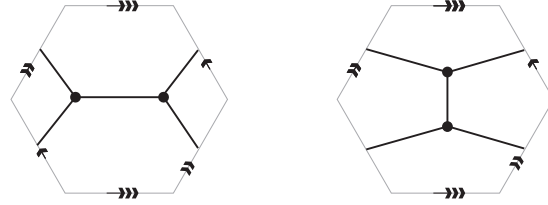


Figure 17: Graphs corresponding to  $X$  and  $X'$ .

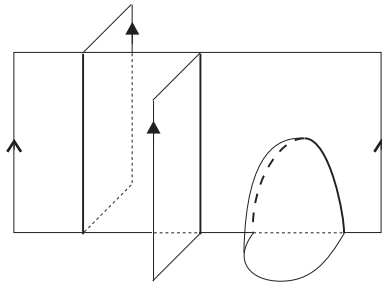


Figure 18: A polyhedron without vertices.

forbidden shape of Fig. 16-left. Our claim is proved. Now note that if  $Y_- \cap \Delta$  has  $\nu$  components then it has  $4 + 2\nu$  free endpoints, which give  $2 + \nu$  vertices in  $P$ . Since  $Y_+$  has 2 vertices and  $Y_-$  has 4, we deduce that  $\nu = 1$  and that  $Q := \text{Cl}(P \setminus \mathcal{R}_P(\Sigma))$  has no vertices. Moreover  $Q$  is connected and standard, and  $\partial Q \cong Y_+ \sqcup Y_-$ . It is not hard to show that with these constraints the only possibility for  $Q$  is as shown in Fig. 18, so  $\partial \mathcal{R}_M(Q)$  has two components. In addition, also  $\Sigma \setminus Y_-$  consists of discs (as  $\Sigma \setminus Y_+$ ), and we get a contradiction because  $\partial \mathcal{R}_M(Q)$  should then be a sphere with some holes.

We are left to analyze the case where  $Y_-$  has two vertices. To show that  $Y_-$  appears as in Fig. 17 it is actually enough to show that  $Y_- \cap \Delta$  is connected and to note that  $Y_-$  must intersect any arc properly embedded in  $\Delta$  and having ends which are the same in  $Y_+$  (otherwise this arc would give a bounding length-1 loop in  $P$ , but  $P$  is minimal).

Suppose by contradiction that  $Y_- \cap \Delta$  is disconnected. Then there exists an arc  $\alpha$  properly embedded in  $\Delta$  which separates two components of  $Y_- \cap \Delta$ . Let us consider the endpoints of  $\alpha$ . By minimality of  $P$ , they cannot belong to the same edge of  $\Delta$ , nor to two adjacent ones, otherwise we could make  $Y_-$  slide on  $\Sigma$  and reduce the number of vertices, as in Fig. 19. The ends of  $\alpha$  also cannot belong to two edges adjacent to one and the same edge, as in Fig. 20-left. To see this, consider



Figure 19: Moves reducing complexity.

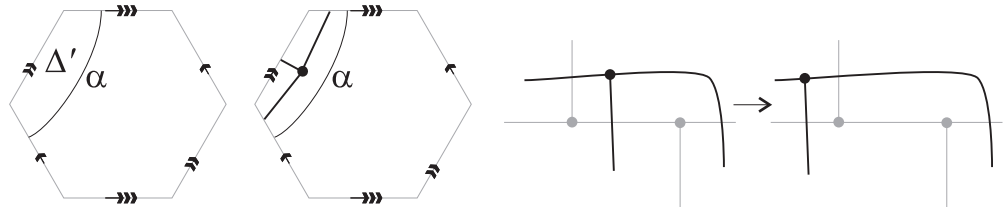


Figure 20: More moves reducing complexity.

how many vertices of  $Y_-$  can lie in  $\Delta'$ . If there are no vertices at all, then either a region of  $P$  contained in  $\Delta'$  has less than 4 vertices or there is a square as in Fig. 16-right. If  $Y_-$  has both vertices in  $\Delta'$ , then again  $\Delta'$  contains either a small region or a forbidden square. These cases are absurd, so there is one vertex of  $Y_-$  in  $\Delta'$ , and the only possible case is shown in Fig. 20-center. On the right in the same figure we show the effect of a T-move which (leaving unaffected everything else, in particular the previous surfaces) creates one of the forbidden squares.

We are left to show that the endpoints of  $\alpha$  also cannot belong to opposite edges of  $\Delta$  (Fig. 21-left). Denote by  $\nu$  and  $\nu'$  the number of ends of  $Y_- \cap \Delta$  on  $e \cap \Delta'$  and on  $e' \cap \Delta'$  respectively. If  $\nu = \nu'$  then  $\alpha$  can be isotoped so to give rise to a length-1

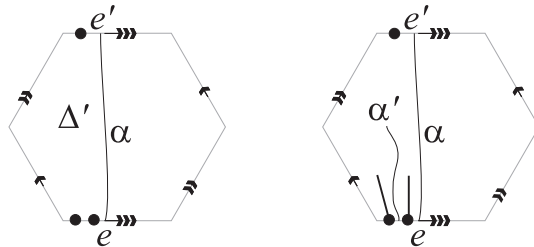


Figure 21: Conclusion of Step 3.

loop in  $P$  bounding an external disc: a contradiction. If  $\nu = 0$  or  $\nu' = 0$  then we can replace  $\alpha$  by a curve disjoint from  $Y_-$  and having ends on edges of  $\Delta$  which are not opposite, so we get back to a case already ruled out. So up to permutation we can assume that  $\nu \geq 2$ . Now the region of  $P$  containing the portion of arc  $\alpha'$  shown in Fig. 21-right must meet another edge of  $Y_+ = \partial\Delta$ , otherwise it is either small or forbidden (recall that  $Y_-$  has 2 vertices only). So  $\alpha'$  extends to a properly embedded arc disjoint from  $Y_-$ . Either  $\alpha'$  belongs to a case already ruled out, or the corresponding  $\nu + \nu'$  is smaller, and a contradiction is reached anyway. This eventually shows that  $Y_-$  is connected, and Step 3 is proved.

**Step 4. De-assembling along the co-disconnecting surface and triods.** Consider the standard polyhedron with boundary  $Q = \text{Cl}(P \setminus \mathcal{R}_P(\Sigma_{\mathcal{T}}))$ , and note that  $Q$  properly embeds in the split manifold  $M_{\Sigma_{\mathcal{T}}}$ . Moreover  $M_{\Sigma_{\mathcal{T}}} \setminus (Q \cup \partial M_{\Sigma_{\mathcal{T}}}) \cong M \setminus P \cong B^3$ , because removing  $\text{int}(\mathcal{R}_M(\Sigma_{\mathcal{T}}))$  or  $\Sigma_{\mathcal{T}}$  from  $M$  is the same. In particular  $Q$  is connected and bounded by an even number of triods, so we can attach to these triods 1-tongued Möbius strips, and the result is a standard spine  $P'$  of a manifold  $M'$  obtained by Dehn-filling all boundary components of  $M_{\Sigma_{\mathcal{T}}}$ . Using now Lemma 3.5 we see that  $(\mathcal{T} \cup \mathcal{L}) \cap \Sigma_{\mathcal{T}} = \emptyset$ , so  $\mathcal{T}$  and  $\mathcal{L}$  survive in  $P'$ . We define  $\mathcal{T}'$  as the set of those elements of  $\mathcal{T}$  which are not parallel to boundary components of the  $\mathcal{R}(\Sigma_{\tau})$ 's, and  $\mathcal{L}'$  as the union of  $\mathcal{L}$  with the cores of the Möbius strips attached. Of course  $(M', P', \mathcal{L}', \mathcal{T}')$  is a pre-system, and it is a system by Remark 3.1, because in the corresponding split spine we have just removed some small tori and added some 1-tongued Möbius strips. By construction  $(M, P, \mathcal{L}, \mathcal{T})$  is obtained from  $(M', P', \mathcal{L}', \mathcal{T}')$  via self-assembling. Proposition 3.10 shows that  $(M', P', \mathcal{L}', \mathcal{T}')$  is fundamental.

By construction for all  $\tau \in \mathcal{T}'$  the torus  $T(\tau)$  is now a separating one in  $M'$ . So we can cut  $P'$  along  $\tau$ , and then glue two 1-tongued Möbius strips to the two resulting polyhedra. This corresponds to cutting  $M'$  along  $T(\tau)$  and then Dehn-filling the boundary components of the two resulting manifolds. If we do this at the same time for all  $\tau \in \mathcal{T}'$  we get spines  $P_1, \dots, P_k$  of closed manifolds  $M_1, \dots, M_k$ . In each  $P_i$  we consider the system  $\mathcal{L}_i$  of the curves of  $\mathcal{L}'$  which lie in  $P_i$ , together with the cores of the Möbius strips contained in  $P_i$ . By construction each  $(M_i, P_i, \mathcal{L}_i, \emptyset)$  is a pre-system, and it is a system by Remark 3.1 (the corresponding split spines only differ for the presence of some 1-tongued Möbius strip). Moreover  $(M', P', \mathcal{L}', \mathcal{T}')$  is an assembling of the  $(M_i, P_i, \mathcal{L}_i, \emptyset)$ 's. Proposition 3.10 now implies that each  $(M_i, P_i, \mathcal{L}_i, \emptyset)$  is fundamental, so it is a brick, and the proof is complete.  $\square$

## 5 Properties of bricks

**Proposition 5.1.** *Let  $\Gamma = (M, Q, \mathcal{L}, \emptyset)$  be a brick. Let  $D$  be an external disc with  $\partial D$  a free loop. Then all regions in  $\Sigma_D$  are discs, and by adding  $D$  and removing any such region we perform a system-move.*

*Proof.* By Lemma 3.5 the surface  $\Sigma_D$  is free; therefore all regions in  $\Sigma_D$  are discs by Proposition 3.9. Since  $\partial D$  and  $\Sigma_D$  are free, the move transforms  $\Gamma$  in a pre-system, which is a system since  $\mathcal{T} = \emptyset$ .  $\square$

**Corollary 5.2.** *Let  $\Gamma = (M, Q, \mathcal{L}, \emptyset)$  be a brick. Let  $\gamma$  be a free loop with  $l(\gamma) \leq 3$ , bounding an external disc  $D$ . Then  $\gamma$  is fake. In particular,  $l(\gamma)$  cannot be 1.*

*Proof.* Since  $\Gamma$  is a brick, the assertion is true if  $l(\gamma) = 0$ . Suppose then  $l(\gamma) \geq 1$ . By Theorem 2.4 there is a region of  $\Sigma_D$  which is incident to at least  $l(\gamma) + 1$  distinct vertices. By removing it we would get a spine with less vertices, which is absurd since  $\Gamma$  is a brick.  $\square$

**Corollary 5.3.** *Let  $\Gamma = (M, Q, \mathcal{L}, \emptyset)$  be a brick. Then there is no free embedded region in  $Q$  incident 3 or fewer vertices.*

*Proof.* Let  $f$  be such a region; it is a disc by Proposition 3.9. A loop in  $Q$  very close to  $\partial f$  and disjoint from  $\bar{f}$  bounds a disc  $D$  parallel to  $f$ . Moreover  $l(\partial D) \leq 3$  and  $\partial D$  is not fake since  $\Sigma_D \supset f$ ; this is impossible by Corollary 5.2.  $\square$

**Corollary 5.4.** *Let  $\Gamma = (M, Q, \mathcal{L}, \emptyset)$  be a brick. Let  $Y$  be a free trace of an orientable surface  $F$ . Then each edge of  $Y$  has distinct endpoints.*

*Proof.* Suppose  $s$  is an edge of  $Y$  with common endpoints; since  $F$  is orientable, the regular neighborhood of  $s$  in  $F$  is an annulus, so there is a component  $D_0 \subset F \setminus Y$  with  $\partial D_0 = s$ . Then  $\partial D_0$  is a free length-1 loop; this is impossible by the previous corollary.  $\square$

## 5.1 Evolution of traces

We will need to consider in the sequel generic time-dependent evolutions of traces on a quasi-standard spine, and the portions of spine swept by such evolutions. To be precise we will call *generic trace evolution* a pair  $(P, f)$ , where  $P$  is a quasi-standard polyhedron, possibly with boundary, and  $f : P \rightarrow [0, 1]$  is a PL-map such that the level set  $Y_t := f^{-1}(t)$  is a connected trace in  $\text{Int}(P)$  for all times  $t$  except the extremal times  $t = 0, 1$  and finitely many other critical times. We require that the catastrophes taking place at the critical times are the elementary ones shown in Fig. 22, and that only one takes place at each time. At the extremal levels  $t = 0, 1$

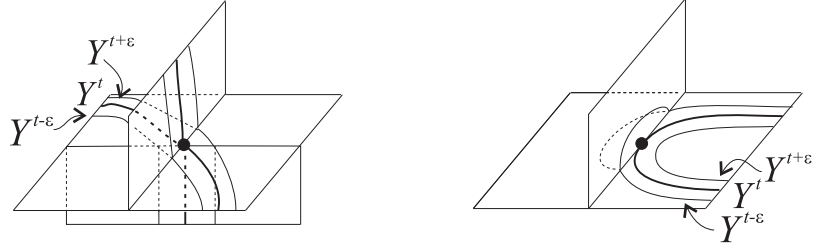


Figure 22: Critical levels.

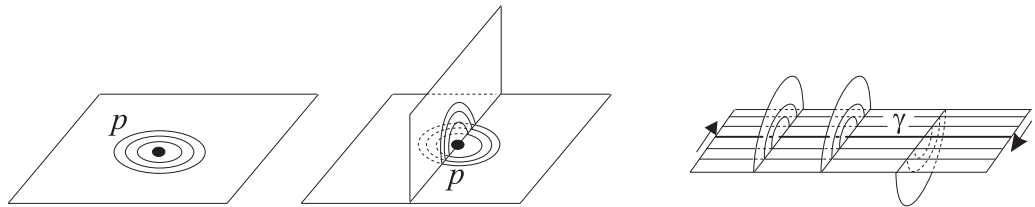


Figure 23: Examples of allowed extremal levels: two points and a loop.

we allow  $Y_t$  to be either a component of  $\partial P$  or a point of  $P$  or a loop in  $P$  (some examples are shown in Fig. 23). We note that if  $Y_0$  (or  $Y_1$ ) is a trace in  $\text{Int}(P)$  then its regular neighborhood is not a product neighborhood, otherwise nearby traces would be disconnected.

If  $(P, f)$  is a generic trace evolution, we will refer to the polyhedron  $P$  equipped with the partition  $\{Y_t\}_{t \in [0,1]}$  with the term *trace-foliated polyhedron*. The “foliation” of  $P$  by traces is of course singular at exceptional and extremal times, but we will use the term foliation anyway, as customary in dimension two.

If  $Q$  is a quasi-standard spine of a closed manifold  $M$  we will call *trace evolution on  $Q$*  a pair  $(P, f)$  as above, with  $P \subset Q$  and  $S(P) = P \cap S(Q)$ . For generic  $t$  the level set  $Y_t$  of  $f$  is the trace of a surface  $F_t$ , and it follows from the definition that the various  $F_t$ ’s are parallel to each other. Moreover if  $P \neq Q$  then  $\partial P \neq \emptyset$  and  $\partial P$  is either  $Y_0$ , or  $Y_1$ , or  $Y_0 \sqcup Y_1$ . If  $\partial P$  is  $Y_0$  or  $Y_1$  then the other extremal level set is either a point or a loop, and  $\cup_{t \in [0,1]} F_t$  is either a ball or a solid torus, whereas if  $\partial P = Y_0 \sqcup Y_1$  then  $\cup_{t \in [0,1]} F_t$  is homeomorphic to  $F_0 \times [0, 1]$ .

Let  $\Gamma = (M, Q, \mathcal{L}, \emptyset)$  be a system. A  $\Gamma$ -foliated subpolyhedron  $P \subset Q$  is a trace-foliated subpolyhedron where every loop  $\gamma \in \mathcal{L}$  is either an extremal level or is disjoint from  $P$ .

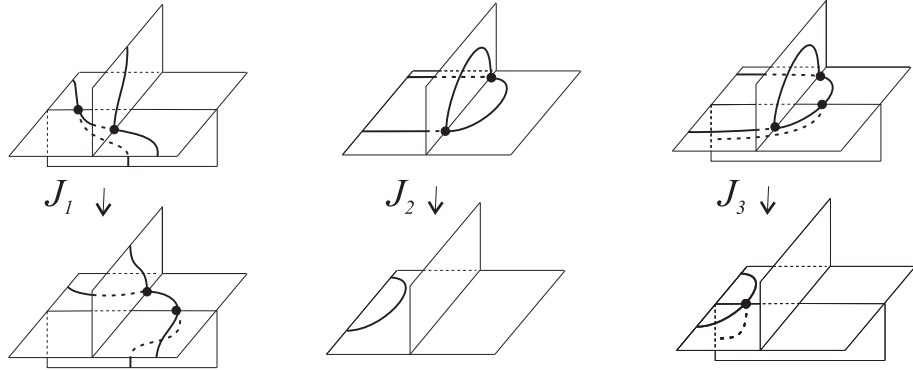


Figure 24: The moves  $J_1, J_2, J_3$ .

**$J$ -moves** Let  $Q$  be a spine of a closed manifold  $M$ . Given the trace  $Y$  of a surface  $F$ , there are some obvious moves that transform  $Y$  into another trace  $Y'$  of a surface  $F'$  isotopic to  $F$ . Three such moves, denoted by  $J_1$ ,  $J_2$  and  $J_3$  and collectively called  $J$ -moves, are shown in Fig. 24. Since we will be concerned with traces of (transversely) orientable surfaces only, we can ask a  $J$ -move to transform a trace  $Y$  into a trace  $Y'$  disjoint from  $Y$ . Let  $[Y, Y']$  be the sub-polyhedron which lies between  $Y$  and  $Y'$ . A sequence of moves  $Y_1 \rightarrow \dots \rightarrow Y_n$  is called a *flow* if each move  $Y_i \rightarrow Y_{i+1}$  is a  $J$ -move (not an inverse  $J$ -move) and  $[Y_{i-1}, Y_i] \cap [Y_i, Y_{i+1}] = Y_i$  for all  $i$ , i.e. if the moves are performed towards the same normal direction to  $Y_i$  for all  $i$ .

**Proposition 5.5.** *Let  $\Gamma$  be a brick. Let  $Y$  be a free trace of an orientable surface. Any flow that starts from  $Y$  defines a  $\Gamma$ -foliated polyhedron.*

*Proof.* Let  $Y'$  be obtained from  $Y$  via a  $J_i$ -move. The polyhedron  $[Y, Y']$  can be trace-foliated: this is easy if  $i = 1, 2$ ; if  $i = 3$  we note that  $J_3$  can be obtained (in two ways) as a composition of one  $J_2$  and one  $J_1$ , so it also has a (non-unique) foliation. Moreover, it is easy to see that  $Y_2$  can be isotoped so that  $[Y, Y']$  is free and therefore  $\Gamma$ -foliated (this property does not hold if we consider the inverse of moves  $J_2, J_3$ !). The assertion follows by iteration.  $\square$

**Remark 5.6.** A move  $J_1$  is determined by an edge  $s$  of  $Y$  and a vertex  $v$  of  $Q$  such that  $s \subset \text{lk}(v)$ , or equivalently by the cone from  $v$  based on  $s$  (a triangle). We will sometimes say that the move is performed *along* the triangle.

**Remark 5.7.** If a move  $J_1$  transforms a trace  $Y$  of  $F$  into a trace  $Y'$  of  $F'$  then there is a natural bijection between the regions of  $F \setminus Y$  and those of  $F' \setminus Y'$ .

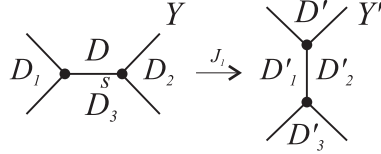


Figure 25: A move  $J_1$  at the level of traces.

Let  $Y$  be the trace of a surface  $F$ . Given a component  $D$  of  $F \setminus Y$ , we denote by  $e(D)$  the number of edges of  $Y$  adjacent to  $D$ , counted with multiplicity (*i.e.* an edge of  $Y$  is counted twice if it has  $D$  on both sides). If there is a component  $D \subset F \setminus Y$  with  $e(D) \leq 3$ , then it is easy to see that  $\partial D$  is a loop (*i.e.*  $\partial_2 D = \emptyset$ ). If  $\partial D$  is fake, then  $e(D) = l(\partial D) = 2, 3$  and a move  $J_{e(D)}$  can be performed.

**Lemma 5.8.** *Let  $\Gamma = (M, Q, \mathcal{L}, \mathcal{T})$  be a brick. Let  $Y$  be a free trace of an orientable surface  $F$ , and let  $D$  be a region of  $F$ . Consider a move  $J_1$  determined by an edge  $s \subset \partial D$  of  $Y$  and a vertex  $v$  of  $Q$ , call  $Y'$  the resulting trace and  $D'$  the disc corresponding to  $D$ . Then  $e(D') < e(D)$  if  $e(D) < 6$  and  $e(D') \leq e(D)$  if  $e(D) = 6$ .*

*Proof.* The trace  $Y'$  is obtained from  $Y$  as shown in Fig. 25; it follows from the figure that if  $e(D') > e(D)$  then  $D_1 = D_2 = D \neq D_3$  and if  $e(D') = e(D)$  then  $D = D_1$  or  $D = D_2$ . By Corollary 5.4 the edges of  $Y$  have distinct ends. Using this fact one easily sees that  $e(D) > 6$  if  $D_1 = D_2 = D \neq D_3$  and  $e(D) \geq 6$  if  $D = D_1$ , and the conclusion follows.  $\square$

Let  $Y$  be a trace of a surface  $F$ . We say that a region  $D \subset F \setminus Y$  is *good* if all regions in  $F \setminus Y$  other than  $D$  are contained in the same component of  $M \setminus (Q \cup D)$ .

**Remark 5.9.** If  $F$  has 2 regions then these regions are good.

**Remark 5.10.** If  $F$  is orientable, then  $\mathcal{R}_Q(Y) \cong Y \times [-1, 1]$ . Recall also from Proposition 2.11 that  $\partial \Sigma_D = \partial_1 D \subset Y$ . Now it is not hard to show that  $D$  is good if and only if the identification  $\mathcal{R}_Q(Y) \cong Y \times [-1, 1]$  can be chosen so that  $\Sigma_D \cap \mathcal{R}_Q(Y) \cong \partial_1 D \times [0, 1]$ . In other words, when  $F$  is orientable we have that  $D$  is good if and only if  $\Sigma_D$  lies on a definite side of  $Y$  in  $Q$ .

**Lemma 5.11.** *Under the assumptions of Lemma 5.8, suppose that  $D$  is good and that  $\Sigma_D$  and the triangle  $sv$  lie on the same side of  $Y$  in  $Q$ . Then  $D'$  is good and  $\Sigma_{D'} = \Sigma_D \setminus [Y, Y']$ .*

*Proof.* The condition that  $\Sigma_D$  and  $sv$  lie on the same side of  $Y$  means that  $Y$ , during its transformation into  $Y'$ , is pushed towards  $\Sigma_D$ , and the conclusion is obvious.  $\square$

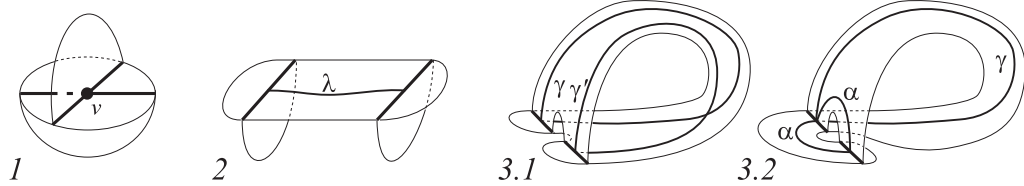


Figure 26: Types 1, 2, 3.1, 3.2. In types 3 the two portions of edge are on the same edge in  $Q$ .

## 5.2 Free traces with 2 and 4 vertices in a brick

**Theorem 5.12.** *Let  $\Gamma = (M, Q, \mathcal{L}, \emptyset)$  be a brick. Let  $Y$  be a free trace of an orientable surface  $F$ . Assume that  $Y$  has 2 vertices. Then  $Q_Y$  has two components, one of which is the  $\Gamma$ -foliated polyhedron  $\mathcal{R}(K)$  where  $K$  is either a point in  $S(Q) \setminus V(Q)$  or a loop in  $\mathcal{L}$ .*

*Proof.* By Corollary 5.4,  $Y$  has three edges  $s_1, s_2, s_3$ , each incident to both vertices of  $Y$ . There are two possibilities for the regular neighborhood  $\mathcal{N}(Y)$  of  $Y$  in  $F$ , already shown above in Fig. 10. In the first case  $F$  is a sphere and  $F \setminus Y$  contains three external discs  $D_i$  with  $e(D_i) = 2$ : by Corollary 5.2 the loops  $\partial D_i$  are all fake; thus we have  $Y = \text{lk}(p)$  for some  $p \in S(Q) \setminus V(Q)$ . In the second case  $F$  is a torus, so  $Y$  is a toric triod and the assertion follows since  $\Gamma$  is maximal.  $\square$

In the statement of the next result, and repeatedly in the sequel, we will describe some standard polyhedra with boundary  $P$  by drawing  $\partial\mathcal{R}(S(P))$  in  $\mathbb{R}^3$ . Our convention will always be that if a component of  $\partial\mathcal{R}(S(P))$  is a circle then  $P$  contains a disc bounded by this circle, while if a component of  $\partial\mathcal{R}(S(P))$  is an arc then it is contained in  $\partial P$ . When a region  $f$  of  $P$  is doubly incident to an edge  $e$  of  $S(P)$ , there is a length-1 loop  $\gamma$  contained in  $f \cup e$ , and we encircle  $e$  to suggest the position of  $\gamma$ . It is worth noting before proceeding that not all standard polyhedra with boundary  $P$  are determined by their  $\mathcal{R}(S(P))$ . More precisely,  $\mathcal{R}(S(P))$  determines  $P$  only when every region of  $P$  intersects  $\partial\mathcal{R}(S(P))$  in one (open or closed) arc only (refer to the Möbius strip with 1 tongue for a counterexample). This explains why 3-dimensional pictures must be employed in some cases.

**Theorem 5.13.** *Let  $\Gamma = (M, Q, \mathcal{L}, \emptyset)$  be a brick, and let  $Y \subset Q$  be the trace of an orientable surface. Assume that  $Y$  is free and has 4 vertices. Then  $Q_Y$  has two components, one of which belongs to one of the following types:*

1.  $\mathcal{R}_Q(v)$  for some  $v \in V(Q)$ ;
2.  $\mathcal{R}_Q(\lambda)$  for an arc  $\lambda$  properly embedded in a region of  $Q$ ;

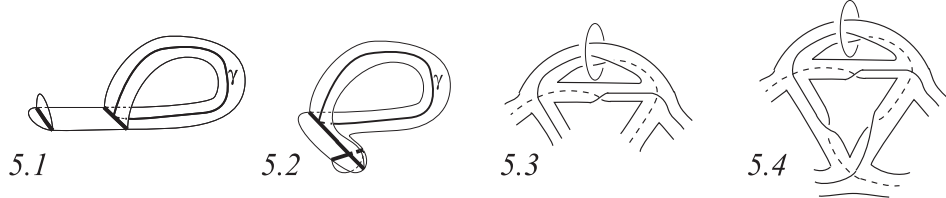


Figure 27: Polyhedra of type 5, with the loop  $\gamma \in \mathcal{L}$  they contain.

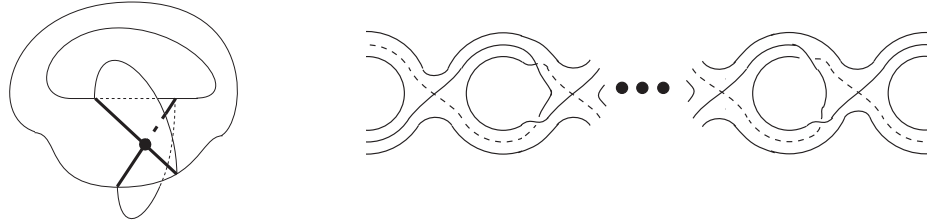


Figure 28: Polyhedra of type 6.

3. Either  $\mathcal{R}_Q(\gamma \cup \gamma')$  where  $\gamma \in \mathcal{L}$ ,  $\gamma'$  is isotopic to  $\gamma$  and  $\gamma \cap \gamma'$  consists of one point away from  $S(Q)$ , or  $\mathcal{R}_Q(\gamma \cup \alpha)$ , where  $\gamma \in \mathcal{L}$ ,  $\alpha$  is a fake length-2 loop, and  $\gamma \cap \alpha$  is a point on  $S(Q)$ ;
4.  $\mathcal{R}_Q(\gamma)$  for a length-2 loop  $\gamma$ , which is fake if it bounds an external disc;
5. One of the 4 polyhedra shown in Fig. 27, each containing a loop  $\gamma \in \mathcal{L}$ , or one of the other 4 polyhedra obtained from one of those of Fig. 27 by removing  $\mathcal{R}_Q(\gamma)$  and gluing it back with some other homeomorphism;
6. A polyhedron as in Fig. 28, with 1 (left) or more (right) vertices;

Moreover:

7. For all types but types 3 the component is  $\Gamma$ -foliated and  $Y$  is the time-1 level. In types 1, 2, 4 and 6 the foliation is disjoint from  $\mathcal{L}$ , while in types 5 the foliation meets  $\mathcal{L}$  precisely at its time-0 level, which is a loop  $\gamma$  belonging to  $\mathcal{L}$  and is shown in Fig. 27;
8. The polyhedra of Fig. 27 are each contained in the next one;
9. Only two types of  $Y$  are possible, as shown in Fig. 29. The polyhedra of types 1, 5.2, 5.3 have boundaries of type A, those of types 2, 3, 5.1, 5.4, 6 have

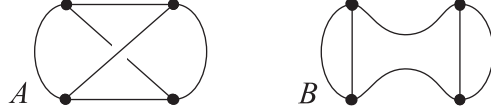


Figure 29: Types  $A$  and  $B$  for  $Y$ .

boundaries of type  $B$ ; a polyhedron of type 4 has boundary of type  $A$  if it is based on a Möbius strip, of type  $B$  otherwise

*Proof.* Our argument is long and organized in many steps. We first describe the overall scheme stating without proof 5 assertions. Later we will provide full proofs. Let  $D \subset F \setminus Y$  be a component having lowest  $e(D)$ .

**Fact 1.** *If  $e(D) \in \{2, 3\}$  then  $Y$  bounds a polyhedron of type 1, 2, 3, 4, 5.1, or 5.2.*

Suppose then that  $e(D) \geq 4$ . Since  $Y$  is trivalent we have  $\chi(F) = d - 2$ , where  $d$  is the number of components of  $F \setminus Y$ . Since  $e(D) \geq 4$  for each component  $D$ , we have  $4d \leq 2e$ , where  $e = 6$  is the number of edges of  $Y$ , so  $d \leq 3$ . It easily follows that  $F$  is a torus and  $d = 2$ . Then  $F \setminus Y$  consists of two discs  $D = D_1, D_2$ , both good by Remark 5.9. Recalling from Corollary 5.4 that all edges of  $Y$  have distinct endpoints one easily sees that only the types  $A$  and  $B$  for  $Y$  are possible. The restriction that  $e(D) \geq 4$  then implies that up to homeomorphism there is only one possible configuration  $(F, Y_A)$  and only one  $(F, Y_B)$ , as shown in Fig. 30. If  $Y$  is of type  $A$  we have  $e(D) = 4$ , otherwise we have  $e(D) = 6$ , and the two regions of  $F$  are completely symmetric. Figure 30 also contains notation used throughout the proof (note that  $s_1, \dots, s_4$  are the edges in  $\partial_1 D$  both in case  $A$  and in case  $B$ ). We know by Proposition 5.1 that  $\Sigma_D \setminus S(Q)$  consists of discs: let  $f_i$  be the disc incident to  $s_i$ . Moreover, let  $g_j$  be the region of  $Q$  incident to  $t_j$ . Since  $D$  is good, we have  $g_1, g_2 \not\subset \Sigma_D$ . Finally, let  $e_i$  be the edge of  $Q$  which contains  $p_i$ .

**Fact 2.** *Either the regions  $f_1, f_2, f_3, f_4, g_1, g_2$  are all distinct or  $Y$  bounds a polyhedron of type 4 or 6.1.*

Assuming that  $Y$  does not bound a polyhedron of type 4 or 6.1, it follows that the segments  $e_i \cap \Sigma_D$  for  $i = 1, \dots, 4$  are distinct. Then let  $v_i \in V(Q)$  be the endpoint of  $e_i \cap \Sigma_D$  not lying on  $D$ .

**Fact 3.** *Up to symmetry we have  $v_1 = v_2$  in case  $A$  and either  $v_1 = v_2$  or  $v_1 = v_3$  in case  $B$ .*

Let us now set  $u = s_1$  in case  $A$ , and either  $u = s_1$  or  $u = t_1$  in case  $B$ , depending on whether  $v_1 = v_2$  or  $v_1 = v_3$ , so there are two edges of  $P \cup D$  which start at the endpoints of  $u$  and both end at  $v_1$ . These edges are  $e'_1 = e_1 \cap \Sigma_D$  and  $e'_m = e_m \cap \Sigma_D$ , with  $m \in \{2, 3\}$  depending on the case. Recall now that if two edges

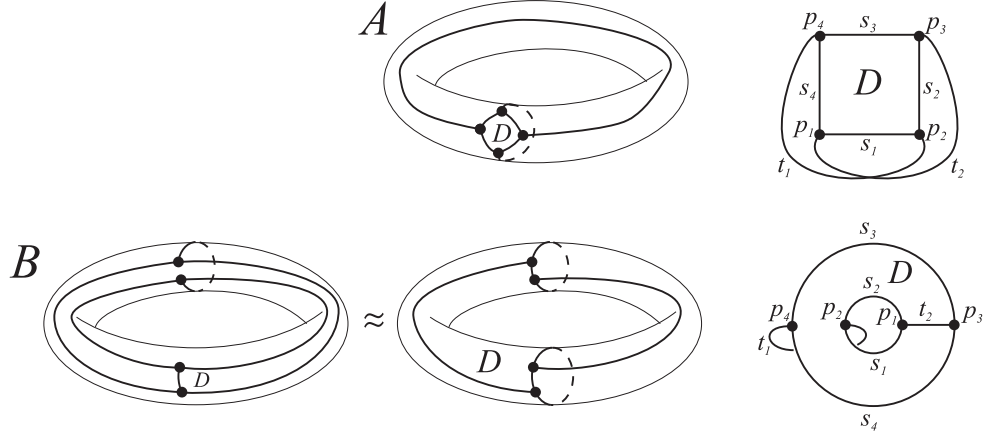


Figure 30: Embeddings of type *A* and *B*.

end at the same vertex then one region incident to the first edge is also incident to the second one. Since we are assuming that the  $f_i$ 's and  $g_j$ 's are distinct, we deduce that  $u \cup e'_1 \cup e'_m$  bounds a region of  $P \cup D$ . Moreover this region is a disc, because either it is contained in  $\Sigma_D$  (in the first two cases) or its boundary is free (in the last case). So the region is triangle, *i.e.*  $u \subset \text{lk}(v_1)$ . Following Remark 5.6 we can then perform a  $J_1$ -move to which Remark 5.9 and Lemma 5.8 apply. Denoting by  $D'$  the disc corresponding to  $D$  after the move, we have  $e(D') \leq e(D)$ , and equality can hold only if  $Y$  is of type *B*.

**Fact 4.** *If  $e(D') < e(D)$ , then  $Y$  bounds a polyhedron of type 5.3 or 5.4.*

**Fact 5.** *If  $e(D') = e(D)$ , then  $Y$  bounds a polyhedron of type 6.2.*

This establishes the theorem. We now prove our assertions.

**Proof of fact 1.** By Corollary 5.2 the loop  $\partial D$  is fake, and we can perform a move  $J_{e(D)}$  as explained in Section 5.1. The result is a free trace  $Y'$  with 2 vertices, so by Theorem 5.12 we have  $Y' = \partial P'$  with  $P' = \mathcal{R}(\gamma)$  or  $P' = \mathcal{R}(p)$ , where  $\gamma$  is a length-1 loop and  $p \in S(Q)$ . It is now not hard to examine all possibilities for  $Y$ . An arrow is sufficient to suggest the inverse  $J_{e(D)}$ -move which takes back from  $Y'$  to  $Y$ , and all essential cases are shown in Fig. 31-left and Fig. 31-center. Arrows 1, 2, 3, 4, 6, and 7 correspond to  $e(D) = 2$ , and arrows 5 and 8 correspond to  $e(D) = 3$ . For arrows 1, 2, 3, 5, 6, and 8, the resulting  $Y$  is respectively of type 3.1, 5.1, 3.2, 5.2, 2, and 1. For arrow 4 the result is shown in Fig. 31-right, and it is of type 5.1 because it is obtained from the polyhedron of Fig. 27-left as explained in the statement. For arrow 7 the result is  $\mathcal{R}(\gamma)$  where  $\gamma$  is a fake length-2 loop.

**Proof of fact 2.** Of course no  $f_i$  can be equal to a  $g_j$ , because  $f_i \subset \Sigma_D$  and

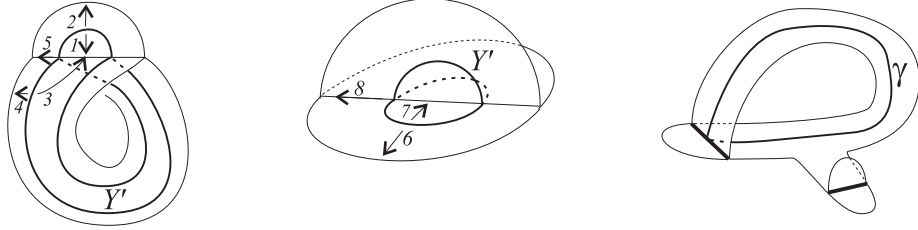


Figure 31: Inverse  $J_{e(D)}$  moves, and one of the possible results.

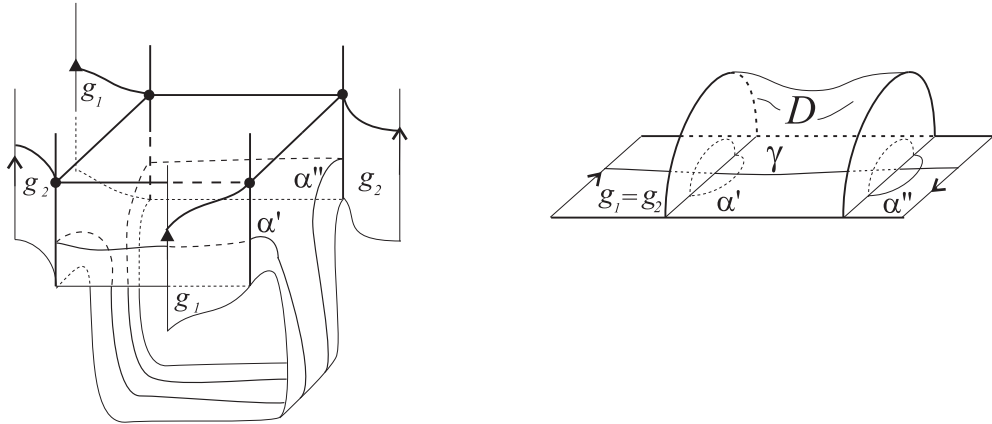


Figure 32: Proof of fact 2: first case.

$g_j \cap \Sigma_D = \emptyset$ . Let us first show that if two  $f_i$ 's coincide then  $Y$  bounds a polyhedron of type 4 or 6.1. We refer to Fig. 30 for the notation.

Assume in case  $A$  that  $f_1 = f_2$ . Join the midpoints of  $s_1$  and  $s_2$  with an arc in  $f_1 = f_2$ , and add half of  $s_1$  and half of  $s_2$  to this arc, obtaining a free length-1 loop  $\alpha$ . Using the fact that  $f_1 = f_2 \subset \Sigma_D$  one readily sees that  $\mathcal{R}(\alpha)$  is an annulus with one tongue. This contradicts Corollary 5.2. So in case  $A$  we cannot have  $f_1 = f_2$ , and similarly in case  $B$  we cannot have  $f_1 = f_2$  or  $f_3 = f_4$ . Up to symmetry, the only cases we are left to deal with are  $A-(f_1 = f_3)$ ,  $B-(f_1 = f_3)$ , and  $B-(f_2 = f_3)$ . In all cases we will show that  $Y$  bounds a polyhedron of type 4 or 6.1. The key point will be to exhibit two loops to which Corollary 5.2 applies.

Case  $A-(f_1 = f_3)$  is examined in Fig. 32-left: since  $\alpha'$  and  $\alpha''$  are fake, one sees quite easily that  $Y = \partial\mathcal{R}(\gamma)$ , where  $\mathcal{R}(\gamma)$  is a Möbius strip with two tongues (Fig. 32-right). Case  $B-(f_1 = f_3)$  is similar (Fig. 33-left); we have  $Y = \partial\mathcal{R}(\gamma)$ , where  $\mathcal{R}(\gamma)$  is an annulus with two tongues on opposite sides (Fig. 33-right). In

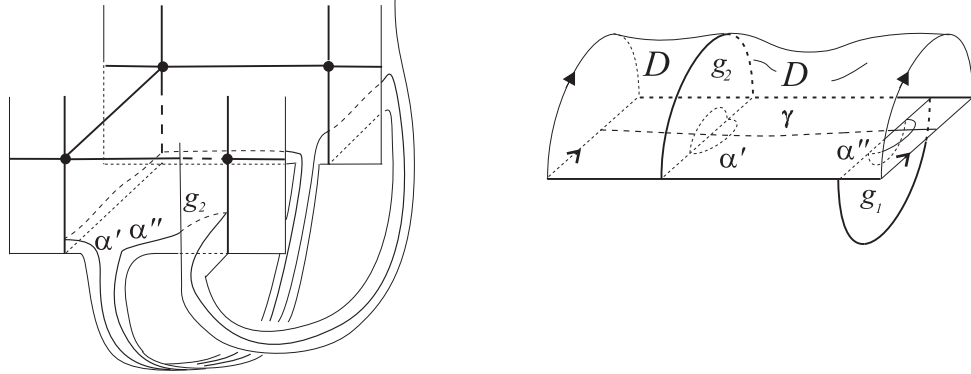


Figure 33: Proof of fact 2: second case.

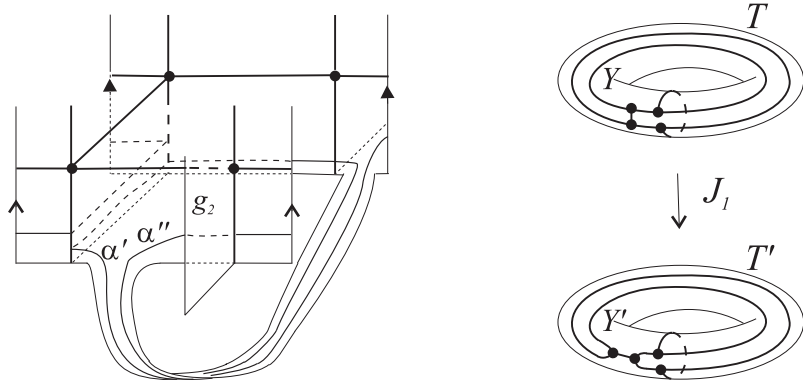


Figure 34: Proof of fact 2: third case.

case  $B$ -( $f_2 = f_3$ ) we consider the loops of Fig. 34-left. Since  $\alpha'$  and  $\alpha''$  are fake we deduce that all the edges  $e_i \cap \Sigma_D$  end at the same vertex  $v$ , such that  $s_2, s_3 \subset lk(v)$ . We can then apply a move  $J_1$  whose effect on  $Y$  is shown in Fig. 34-right. The result is a free trace  $Y'$  which falls into case  $A$ -( $f_1 = f_3$ ). So  $Y' = \partial \mathcal{R}(\gamma)$  with  $\mathcal{R}(\gamma)$  a Möbius strip with two tongues. Recalling that the inverse of a  $J_1$ -move is again a  $J_1$ -move, we only need to consider which such moves can be applied to  $P'$ . The move is determined by the edge of  $\partial P'$  which disappears during the move: of the 6 edges of  $\partial P'$ , 4 lead to a situation in which  $e(D) = 3$ , so we exclude them. The other 2 edges are actually symmetric, and the result is of type 6.1.

To conclude the proof of Fact 2 we must show that if the  $f_i$ 's are distinct then  $g_1 \neq g_2$ . If  $Y$  is of type  $B$  then  $g_1$  has a certain component of  $M \setminus (Q \cup D)$  on both

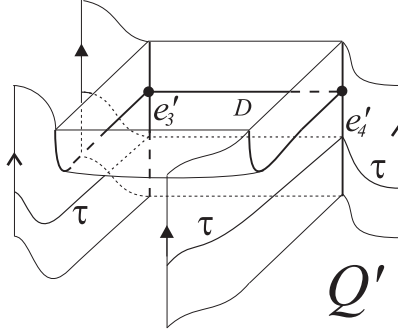


Figure 35: A toric triod  $\tau \subset Q'$  which meets the edges  $e'_3, e'_4$ .

sides, and  $g_2$  has the other one, so  $g_1 \neq g_2$ . Assume in case  $A$  that  $g_1 = g_2$ . Referring to Fig. 30 let  $q_j$  be the midpoint of  $t_j$ , and join  $q_1$  to  $q_2$  by an arc  $\lambda$  in  $g_1 = g_2$ . There are 4 distinct arcs  $\lambda_1, \dots, \lambda_4 \subset Y$  having endpoints  $q_0, q_1$  and intersecting  $S(Q)$  twice. For two of them the polyhedron  $\mathcal{R}(\lambda \cup \lambda_i)$  is an annulus with 2 tongues on the same side. Then some  $\lambda \cup \lambda_i$  is fake, which is in contrast with the fact that the  $f_i$ 's are distinct.

**Proof of fact 3.** We start with case  $A$ . Assume that  $v_1 \neq v_2$ , and let  $Q' = (Q \cup D) \setminus f_1$ . By Remark 5.1 the transformation of  $Q$  into  $Q'$  yields a system-move from  $\Gamma$  to  $\Gamma' = (M, Q', \mathcal{L}, \emptyset)$ . If  $x$  different vertices of  $Q$  are contained in  $\bar{f}_1$  then  $\#V(Q') = \#V(Q) + 4 - 2 - x$ . Since  $\Gamma$  is a brick we have  $x \leq 2$ . On the other hand  $\bar{f}_1$  contains  $v_1$  and  $v_2$ , so  $x = 2$ . Now Fig. 35 shows a toric triod  $\tau$  in  $Q'$ , where  $T(\tau)$  is parallel and very close to  $F$ , so  $\tau$  is free. But  $\Gamma'$  is maximal, so  $\tau = \partial \mathcal{R}_{Q'}(\gamma)$  for some  $\gamma \in \mathcal{L}$ . In particular  $e'_3 = e'_4$  in  $Q'$ , which implies that  $\{v_3, v_4\} \subset \bar{f}_1$ , i.e.  $\{v_3, v_4\} \subset \{v_1, v_2\}$ . So either  $v_3 = v_4$ , or  $v_4 = v_1$ , or  $v_3 = v_1 \neq v_4 = v_2$ . In all cases but the last one the conclusion is the desired one up to symmetry. Concentrating on the last case, we note that  $f_1 \cup \dots \cup f_4$  is a surface near  $v_1$  and  $v_2$ , and that the  $f_i$ 's and  $g_j$ 's are all distinct. From these facts it is not hard to deduce that  $v_1$  and  $v_2$  appear as in Fig. 36. The figure readily implies that  $f_2 = f_4$ : a contradiction.

The proof in case  $B$  is similar, except that  $D$  cannot be used directly: a perturbed version  $D'$  as in Fig. 37-left must be employed. We are again supposing here that  $v_1 \neq v_2$ , so  $\bar{f}_1$  contains  $x \geq 2$  vertices of  $Q$ , but now  $\#V(Q') = \#V(Q) + 6 - 3 - x$ . Since  $Q$  is a brick we have  $x \geq 3$ , so  $x \in \{2, 3\}$ . We first claim that we can suppose  $x = 3$  up to symmetry. By contradiction, assume that both  $\bar{f}_1$  and  $\bar{f}_2$  contain exactly 2 vertices. We deduce that the situation is as in Fig. 37-right, where we also show a length-1 loop bounding an external disc. Being very close to or contained in  $\Sigma_D$ , the

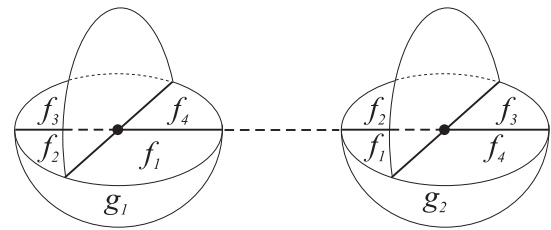


Figure 36: The vertices  $v_1$  and  $v_2$ .

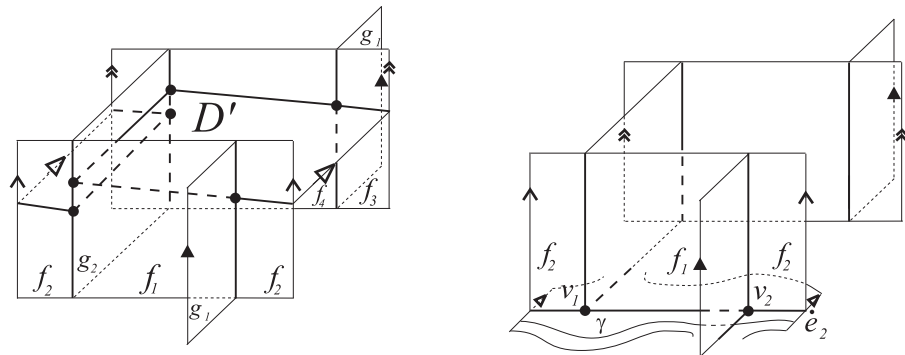


Figure 37: The perturbed disc  $D'$  (left), and a length-1 loop bounding an external disc (right).

loop is free, and we get a contradiction to Corollary 5.2. Our claim that  $x = 3$  up to symmetry is proved, so  $\#V(Q') = \#V(Q)$ . By definition of brick,  $(M, Q', \mathcal{L}, \emptyset)$  is maximal. A figure very similar to Fig. 35 shows that a toric triod must exist in  $Q'$ , and allows to conclude as above that  $\{v_3, v_4\} \subset \overline{f}_1$ . So either  $v_3 = v_4$ , which gives the desired conclusion up to symmetry, or  $\{v_3, v_4\} \cap \{v_1, v_2\} \neq \emptyset$  (recall that  $\overline{f}_1$  contains exactly 3 vertices). If  $v_3 = v_1$  or  $v_4 = v_2$  we get the desired conclusion. Otherwise we can assume up to symmetry that  $v_1 = v_4$ . So  $e_1$  and  $e_4$  have a common vertex in  $Q$ , which implies that there is a region incident to both. But  $e_1$  is adjacent to  $f_1, f_2, g_1$  and  $e_4$  is adjacent to  $f_3, f_4, g_2$ , and the  $f_i$ 's and  $g_j$ 's are distinct, so we get a contradiction.

**Proof of fact 4.** If  $Y$  is of type  $A$ , then  $e(D') = 3$ , so by Fact 1 (and its proof)  $Y'$  bounds a  $\Gamma$ -foliated polyhedron  $P'$  of type 5.2 or of type 1, but the latter is impossible because  $Y'$  is the trace of a torus. We only need to consider which  $J_1$ -moves can be applied to a  $P'$  of type 5.2. By Remark 5.11 the move actually takes place towards the exterior of  $P'$  (*i.e.* its result contains 2 vertices of  $Q$ ). The move is determined by the edge of  $\partial P'$  which disappears during the move: of the 6 edges in  $\partial P'$ , 3 lead to a situation in which  $e(D) = 2$ , so we exclude them. The other 3 edges are actually symmetric up to removing  $\mathcal{R}(\gamma)$  and gluing it back, and the result is one of the polyhedra of type 5.3.

If  $Y$  is of type  $B$ , then  $u$  must be an edge in  $\partial_2 D$  (otherwise  $e(D') = e(D)$ ), so  $Y'$  is of type  $A$ . Moreover  $Y'$  is the trace of a torus. Combining Fact 2 and the part of Fact 4 already established we see that  $Y' = \partial P'$  with  $P'$  either of type 5.3 or of type 4 based on a Möbius strip. However, if we denote by  $f'_i$  the faces of  $\Sigma_{D'}$  incident to  $D'$ , we have  $f'_i \subset f_i$  up to permutation, so the  $f'_i$ 's are distinct. This shows that type 4 is impossible, and again we are left to analyze what can we get from a  $P'$  of type 5.3 by a move  $J_1$  which takes place towards the exterior. Of the 6 edges of  $\partial P'$ , 4 lead to a situation in which  $e(D) = 3$ , so we exclude them. The other 2 edges are actually symmetric, and the result is type 5.4.

**Proof of fact 5.** The first step of our proof is the extension of the move  $Y \rightarrow Y'$  to a flow  $Y \rightarrow Y' \rightarrow Y'' \rightarrow \dots \rightarrow Y^{(k)}$  of  $J_1$ -moves. As mentioned in the proof of Fact 4 we must have  $u \subset \partial_1 D$  in this case, so we assume up to symmetry that  $u = s_1 \subset \partial f_1$ , and we note that Remarks 5.9–5.11 apply. The situation is described in Fig. 38. One easily sees that the regions of  $\Sigma_{D'}$  incident to  $\partial_1 D'$  are  $f_3, f_4$  and two new ones (one of which is contained in  $f_2$ ), which we denote by  $f'_1, f'_2$ . If  $\{f'_1, f'_2, f_3, f_4\}$  are not distinct, the flow is reduced to  $Y \rightarrow Y'$ , and we move to the next step. Otherwise let  $v'_1, v'_2$  be the ends of  $e'_1, e'_2$  (see Fig. 38-left). If  $v'_1 \neq v'_2$  then again the flow is reduced to  $Y \rightarrow Y'$ . Assume on the contrary that  $v'_1 = v'_2$ , and consider Fig. 38-right. Then either  $s'_1$  or  $s'_2$  is contained in  $\text{lk}(v')$ , but certainly  $s'_1$  is not, for otherwise  $Q$  would contain a free embedded region with two vertices, which is absurd by Corollary 5.3.

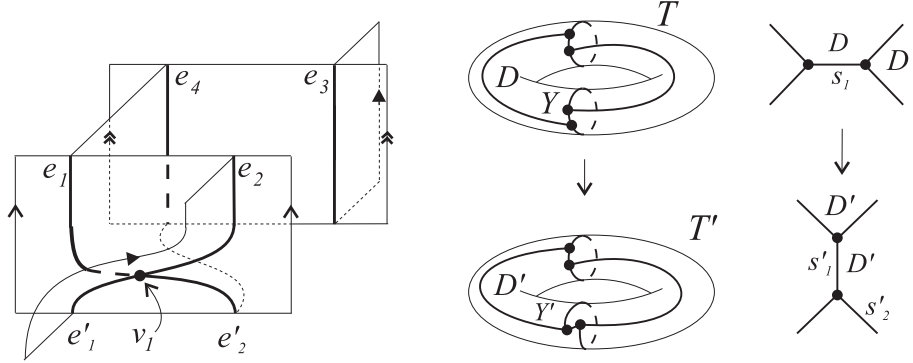


Figure 38: Proof of Fact 5.

Setting  $u' = s'_2$ , we are now in a position to apply a move  $J_1$  along the triangle determined by  $v'_1$  and  $u'$ , getting from  $Y'$  to  $Y''$ . We proceed in a similar way and note that the process must come to an end because  $\Sigma_{D^{(i)}}$  contains one vertex less than  $\Sigma_{D^{(i-1)}}$  by Remark 5.11.

Our second step is to understand the final stage  $Y^{(k)}$  of our flow. By construction either  $\{f_1^{(k)}, f_2^{(k)}, f_3, f_4\}$  are not distinct or  $v_1^{(k)} \neq v_2^{(k)}$ . In the first case, since at each step only 1 region not contained in the previous one is inserted (and 1 is deleted), precisely 3 of  $\{f_1^{(k)}, f_2^{(k)}, f_3, f_4\}$  are distinct. We know by Fact 2 (and its proof) that  $Y^{(k)}$  (which is of type B) bounds a polyhedron  $P$  which is either an annulus with 2 tongues on opposite sides, or of type 6.1. The first case is excluded by what just said about the  $f_i$ 's. By Remark 5.11,  $Y$  bounds  $P \cup_{Y^{(k)}} [Y, Y^{(k)}]$ . Since at each step of the construction of our flow the choice of move  $J_1$  was forced, the polyhedron  $[Y, Y^{(k)}]$  is defined unambiguously (it depends on  $k$  only). We only need to explain which edge of  $\partial P$  determines the  $J_1$ -move which glues  $P$  to  $[Y, Y^{(k)}]$ . Of the 6 edges, 2 lead to a trace of type A, 2 give rise to a free embedded face with 2 edges (excluded by Corollary 5.3) and the other 2 are symmetric, so  $P \cup_{Y^{(k)}} [Y, Y^{(k)}]$  also depends on  $k$  only. It is now a routine matter to check that indeed  $P \cup_{Y^{(k)}} [Y, Y^{(k)}]$  is the polyhedron of type 6 with  $k$  vertices.

Having understood the case where  $\{f_1^{(k)}, f_2^{(k)}, f_3, f_4\}$  are not distinct, we assume that they are. The rest of the proof is devoted to showing that it is actually impossible that  $v_1^{(k)} \neq v_2^{(k)}$ . Let us first assume that  $v_3 \neq v_4$ . By Fact 3 we then have  $v_1 = v_3$  up to symmetry, and we can apply a move  $J_1$  which reduces  $e(D)$ . Fact 4 shows that  $Y^{(k)}$  bounds a polyhedron  $P$  of type 5.3 or 5.4, but  $\partial P$  is of type B, so it must be of type 5.4. Once again we must analyze the possible results of a move  $J_1$ , towards the exterior of a  $P$  of type 5.4. Of the 6 edges of  $\partial P$ , 2 lead to a

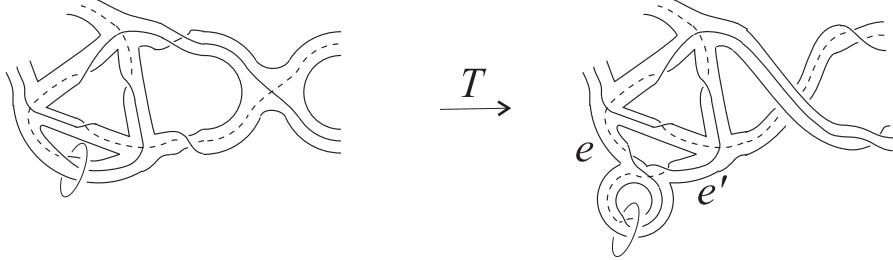


Figure 39: Proof of Fact 5 continued.

trace of type  $A$ , and therefore are excluded. The 4 other edges come in 2 symmetric pairs. For one type, the result of the move  $J_1$  contains a free embedded region with 3 vertices, which is absurd by Corollary 5.3. The other possible result is shown in Fig. 39-left. We have in this case a free embedded region with 4 vertices, to which a  $T$ -move can be applied. The result is shown in Fig. 39-right. In this polyhedron there is a 1-bridge  $(e, e')$  and a 2-vertex trace orthogonal to it, and we easily get a contradiction to Theorem 5.12.

We are left to deal with the case where  $\{f_1^{(k)}, f_2^{(k)}, f_3, f_4\}$  are distinct,  $v_1^{(k)} \neq v_2^{(k)}$ , and  $v_3 = v_4$ . In this case we can perform a  $J_1$ -move along either  $s_3$  or  $s_4$ , and we can proceed just as above, constructing a flow  $Y^{(k)} \rightarrow Y^{(k+1)} \rightarrow \dots \rightarrow Y^{(k+h)}$ . During this process the faces  $f_1^{(k)}, f_2^{(k)}$ , and the vertices  $v_1^{(k)}, v_2^{(k)}$  remain unaffected, while  $f_3, f_4, v_3 = v_4$  get transformed into  $f_3^{(h)}, f_4^{(h)}, v_3^{(h)}, v_4^{(h)}$ . As above, we have at the end of the sequence either that  $\{f_1^{(k)}, f_2^{(k)}, f_3^{(h)}, f_4^{(h)}\}$  are not distinct or that  $v_3^{(h)} \neq v_4^{(h)}$ . In the first case, Fact 2 implies that  $Y^{(k+h)}$  bounds a polyhedron of type 4 or 6.1. Such a polyhedron has at most 1 vertex, but  $\Sigma_{D^{(k+h)}}$  contains at least  $v_1^{(k)} \neq v_2^{(k)}$ , and we get a contradiction. In the second case we are precisely in the situation  $v_3 \neq v_4$  previously considered, and again we get a contradiction.  $\square$

### 5.3 Further properties

Given a spine  $Q$  and a length-1 loop  $\gamma$ , let  $\epsilon(\gamma)$  be the edge of  $Q$  intersecting  $\gamma$ . Besides  $\Theta_0$ , two bricks needed below are defined as

$$\begin{aligned}\Theta_1 &= (L_{4,1}, B_1, \{\gamma_1^1, \gamma_2^1\}, \emptyset), \\ \Theta_2 &= \left( (S^2, (2,1), (2,1), (2,1), (1,-1)), B_2, \{\gamma_1^2, \gamma_2^2, \gamma_3^2\}, \emptyset \right),\end{aligned}$$

where the polyhedra  $B_1, B_2$  are standard, and regular neighborhoods their 1-skeleta are shown in Fig. 40; the loops  $\gamma_i^j$  are uniquely determined by the edges  $\epsilon(\gamma_i^j)$ ,

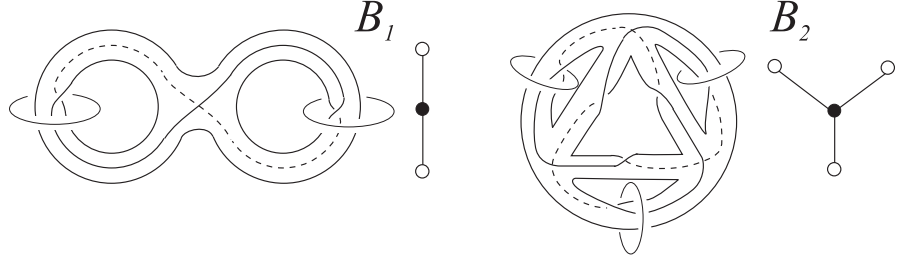


Figure 40: Neighborhoods of the 1-skeleta of the bricks  $\Theta_1$  and  $\Theta_2$ .

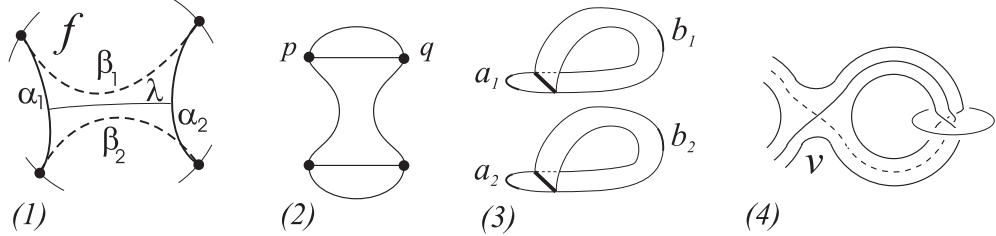


Figure 41: Proof of Proposition 5.14.

encircled in the figure. The loops  $\gamma_1^1, \gamma_2^1$  are the cores of the genus 1 Heegaard splitting of  $L_{4,1}$ ; the loops  $\gamma_1^2, \gamma_2^2, \gamma_3^2$  are the exceptional fibers of the Seifert manifold having normalized parameters  $(S^2, (2, 1), (2, 1), (2, 1), (1, -1))$ . The proof that these maximal systems are indeed bricks can be easily made by hand.

**Proposition 5.14.** *Let  $\Gamma = (M, Q, \mathcal{L}, \emptyset)$  be a brick. Assume  $\mathcal{L} = \{\gamma_1, \dots, \gamma_k\}$ . For  $\gamma_i \in \mathcal{L}$ , let  $f_i^1$  be the region of  $Q$  whose closure contains  $\gamma_i$ , and let  $f_i^2$  be the other region of  $Q$  incident to  $\epsilon(\gamma_i)$ . If  $\Gamma$  is not similar to  $\Theta_0, \Theta_1$  or  $\Theta_2$ , then the faces  $\{f_1^1, f_1^2, \dots, f_k^1, f_k^2\}$  are all distinct.*

*Proof.* Let us consider the disjoint triods  $Y_i = \partial \mathcal{R}(\gamma_i)$ . A region  $f$  of  $Q$  intersects  $\cup_i Y_i$  in some properly embedded arcs; suppose by contradiction that there is an  $f$  which either intersects at least two distinct  $Y_i$ 's, or intersects a certain  $Y_i$  in three arcs. Then there are arcs in  $(\cup_i Y_i) \cap f$ , say  $\alpha_1, \alpha_2$ , with the property that there is an embedded arc  $\lambda$  in  $f$  with endpoints  $\lambda_1 \in \alpha_1$  and  $\lambda_2 \in \alpha_2$  and with interior disjoint from all  $\gamma_i$ 's. Each  $\lambda_j$  belongs to a triod  $Y_{i_j}$ . Let  $Y$  be the trace obtained from  $Y_{i_1} \cup Y_{i_2}$  by replacing  $\alpha_1 \cup \alpha_2$  with two arcs  $\beta_1 \cup \beta_2$  as in Fig. 41-(1). By construction the trace  $Y$  is free.

Suppose  $Y_{i_1} \neq Y_{i_2}$ , and assume  $i_1 = 1, i_2 = 2$ . Then  $Y$  is as in Fig. 41-(2)

and  $Q_Y = Q_1 \sqcup Q_2$ , with  $Q_2$  obtained from  $\mathcal{R}(\gamma_1) \sqcup \mathcal{R}(\gamma_2)$  by identifying an arc in  $\partial\mathcal{R}(\gamma_1)$  to one in  $\partial\mathcal{R}(\gamma_2)$ . Note that  $\overline{f}$  may or not contain  $\gamma_1$ , and similarly for  $\gamma_2$ . Depending on whether it does or not,  $Q_2$  is obtained from the strips of Fig. 41-(3) under one of the following gluings: either  $a_1 \cong a_2$ , or  $b_1 \cong b_2$ , or  $a_1 \cong b_2$  (of course  $b_1 \cong a_2$  gives the same result, and orientations are always immaterial). Now Proposition 2.6 implies that  $Y$  is the trace of an orientable surface. Then either  $Q_1$  or  $Q_2$  is of one on the types listed by Theorem 5.13: no such type is homeomorphic to  $Q_2$ , since  $Q_2$  contains two disjoint length-1 loops. Therefore  $Q_1$  must be of one such type. The only polyhedra among those listed in Theorem 5.13 having at least one vertex and boundary homeomorphic to the graph in Fig. 41-(2) are those of type 5.4 (Fig. 27) and 6 (Fig. 28). If  $Q_1$  is of type 5.4 then  $P_\Gamma = P_{\Theta_2}$ , if  $Q_1$  is of type 6 with 1 vertex then  $P_\Gamma = P_{\Theta_1}$ , so  $\Gamma$  is similar either to  $\Theta_2$  or to  $\Theta_1$  and we are done. Otherwise  $Q_1$  is of type 6 with  $k \geq 2$  vertices. Now, with labels as in Fig. 41-(3), we have in  $Q_1$  an arc of  $\epsilon(\gamma_1)$  joining  $p$  and  $q$ , whereas in  $Q_2$  the edges through  $p$  and  $q$  end at the same vertex  $v$ . So  $\epsilon(\gamma_1)$  appears as in Fig. 41-(4). Moreover there is an edge  $s$  of  $\partial\mathcal{R}(\gamma_1)$  which lies in  $\text{lk}(v)$ . Applying the move  $J_1$  determined by  $s$  and  $v$  we get a non-loop-like toric triod disjoint from  $\mathcal{L}$ , which contradicts the definition of brick.

Now suppose  $Y_{i_1} = Y_{i_2}$ , and let  $i_1 = 1$ . So  $Y$  has 2 vertices, and  $Q_Y = Q_1 \sqcup Q_2$ , with  $Q_2$  obtained from the first strip of Fig. 41-(3) identifying  $a_1$  to  $b_1$ . Using Theorem 5.12 we deduce that  $Q_1$  must be a neighbourhood of a singular point or of a loop  $\gamma \in \mathcal{L}$ . In both cases we see that  $Q = B^0$ , so  $\Gamma = \Theta_0$ .  $\square$

**Proposition 5.15.** *Every brick with at least 1 vertex is standard.*

*Proof.* Let  $\Gamma = (M, Q, \mathcal{L}, \emptyset)$  be the brick. We only need to show that the regions of  $Q$  are discs. By Proposition 3.9  $P_\Gamma$  is standard, and by Proposition 5.14 each region of  $Q$  intersects at most one element of  $\mathcal{L}$ . So, if a region  $f$  is not a disc, then  $\overline{f}$  contains one  $\gamma \in \mathcal{L}$ , and  $f$  is either an annulus (with  $\gamma$  joining its two boundary components) or a Möbius strip. In both cases we can find a length-0 loop  $\alpha \subset f$  such that  $\alpha \cap \gamma = \{p\}$ . Now  $Y := \partial\mathcal{R}(\alpha \cup \gamma)$  is a free 2-vertex trace of an orientable surface, and  $Q_Y$  has two components  $Q_1$  and  $Q_2 = \mathcal{R}(\alpha \cup \gamma)$ . Since  $Q_2$  is not a regular neighborhood of a point or of a loop then  $Q_1$  must be by Theorem 5.12, but then  $V(Q)$  would be empty, which was excluded by assumption.  $\square$

Since it is easy to see that a standard polyhedron can sit in a finite number of non-isomorphic systems (see the first step of Theorem 4.2), the previous result together with Fact 3.11 implies that for each  $n \geq 0$  there is a finite number of bricks with  $n$  vertices. It is then possible to prove by checking all standard spines with at most 3 vertices the following:

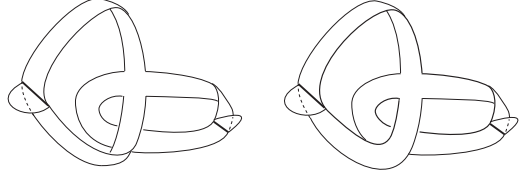


Figure 42: The polyhedron  $\mathcal{R}(\gamma \cup \gamma')$  if  $\gamma$  bounds a disc (left) and if it does not (right).

**Fact 5.16.** *Each brick having at most 3 vertices and containing some length-1 loop is similar to  $\Theta_0$ ,  $\Theta_1$ , or  $\Theta_2$ .*

**Lemma 5.17.** *Let  $\Gamma = (M, Q, \mathcal{L}, \emptyset)$  be a brick with at least 4 vertices. Then each length-1 loop  $\gamma \subset Q$  is isotopic to an element of  $\mathcal{L}$ .*

*Proof.* The loop  $\gamma$  cannot be free: if it bounds a disc by Corollary 5.2, if not because  $\mathcal{L}$  is maximal. So let  $\gamma' \in \mathcal{L}$  meet  $\gamma$ . Of course we can assume that  $\gamma' \cap \gamma$  is one point away from  $S(Q)$ . Now let  $f$  be the face of  $Q$  whose closure contains  $\gamma$ . By Proposition 5.14  $\gamma'$  is the only element of  $\mathcal{L}$  which meets  $\bar{f}$ . So  $Y := \partial \mathcal{R}(\gamma \cup \gamma')$  is a 4-vertex trace of an orientable surface, and  $Q_Y$  has two components  $Q_1$  and  $Q_2$ , where  $Q_2 = \mathcal{R}(\gamma \cup \gamma')$  is one of the polyhedra shown in Fig. 42.

Then either  $Q_1$  or  $Q_2$  is of one of the types listed in Theorem 5.13. Suppose that  $Q_2$  is: one easily sees that  $Q_2$  cannot be  $\Gamma$ -foliated, so it is of type 3, and  $\gamma$  and  $\gamma'$  are isotopic. Suppose now that  $Q_1$  is as in Theorem 5.13. Now  $Q_2$  cannot be the polyhedron in Fig. 42-left, because the types listed in Theorem 5.13 which have the same boundary as  $Q_2$  have at most 2 vertices. So  $Q_2$  is the polyhedron in Fig. 42-right, and there exists a length-2 loop in  $\partial Q_2$  bounding an external disc (shown in the figure). By Corollary 5.2 such a loop is fake, thus we have  $\epsilon(\gamma) = \epsilon(\gamma')$ ; by Proposition 5.14 the face  $f$  is incident twice to  $\epsilon(\gamma')$ , so  $\gamma$  and  $\gamma'$  are isotopic.  $\square$

Given a quasi-standard polyhedron  $P$ , let  $\mathcal{L}(P)$  be the set of all loops having length 1 contained in  $P$ , up to isotopy.

**Corollary 5.18.** *Let  $Q$  be a standard polyhedron having at least 4 vertices. Then there exists (up to isomorphism) at most one brick of the form  $\Gamma = (M, Q, \mathcal{L}, \emptyset)$ . Moreover  $\mathcal{L}$  is a set of representatives for  $\mathcal{L}(Q)$ .*

*Proof.* Since  $\Gamma$  is not similar to  $\Theta_0$ ,  $\Theta_1$ , or  $\Theta_2$ , Lemma 5.17 implies that  $\mathcal{L}$  is a set of representatives of  $\mathcal{L}(Q)$ , and Proposition 5.14 easily allows to deduce that such a set is unique, and both conclusions follow.  $\square$

We can therefore use a simpler notation: a spine  $Q$  with at least 4 vertices is a *brick* if and only if it is standard and  $(M, Q, \mathcal{L}, \emptyset)$  is a brick, where  $M$  is the unique manifold that has  $Q$  as spine and  $\mathcal{L}$  is any set of representatives for  $\mathcal{L}(Q)$ . Moreover, we denote by  $B_i$  the brick  $\Theta_i = (M_i, B_i, \mathcal{L}_i, \emptyset)$  for  $i = 0, 1, 2$ .

Given a spine  $Q$  and a length-1 loop  $\gamma$ , the edge  $\epsilon(\gamma)$  met by  $\gamma$  depends on the isotopy class of  $\gamma$  only; so the map  $\epsilon$  is well-defined on  $\mathcal{L}(Q)$ .

**Proposition 5.19.** *Let  $Q$  be a brick not similar to  $B_0$ ,  $B_1$ , or  $B_2$ . Then  $\text{Cl}(\epsilon(\gamma_1)) \cap \text{Cl}(\epsilon(\gamma_2)) = \emptyset$  for  $\gamma_1 \neq \gamma_2 \in \mathcal{L}(Q)$ , so  $\#\mathcal{L}(Q) \leq \#V(Q)/2$ .*

*Proof.* By Proposition 5.14,  $\epsilon(\gamma_i)$  is adjacent twice to a region  $f_i^1$  and once to another region  $f_i^2$ , and the faces  $f_i^j$  are distinct. So of course  $\epsilon(\gamma_1) \neq \epsilon(\gamma_2)$ . Moreover they cannot have a common endpoint, because for any two edges having a common vertex there is a region incident to both. The last inequality is obvious.  $\square$

The following proposition says, in Matveev's sense [4], that a generic brick contains no *triple overpass*.

**Proposition 5.20.** *Let  $Q$  be a brick not similar to  $B_0$ ,  $B_1$  or  $B_2$ . Then no edge of  $Q$  meets 3 times the same region.*

*Proof.* Suppose an edge  $e$  meets 3 times a region  $f$ . Then there is a  $\gamma \in \mathcal{L}(Q)$  with  $e = \epsilon(\gamma)$ ; this is absurd by Proposition 5.14.  $\square$

**Proposition 5.21.** *Let  $Q$  be a brick. Then every  $n$ -bridge in  $S(Q)$  has at least one free orthogonal trace.*

*Proof.* If  $Q$  is similar to  $B_0$ ,  $B_1$  or  $B_2$ , the only  $n$ -bridge that can occur is a 2-bridge obtained taking 4 edges incident to the same vertex  $v$ : in this case  $\text{lk}(v)$  is a free orthogonal trace. So we can suppose by Proposition 5.14 that each region of  $Q$  intersects at most one loop in  $\mathcal{L}(Q)$ .

Recall that the construction of an orthogonal trace proceeds independently in each region of  $Q$ , by joining in pairs certain points on the boundary. If  $f$  is such a region, and  $\gamma$  is the only element of  $\mathcal{L}(Q)$  meeting  $f$ , then it is very easy to see that the points on  $\partial f$  are separated into two even subsets by  $\gamma$ , so they can be joined away from  $\gamma$ .  $\square$

**Corollary 5.22.** *If  $Q$  is a brick, then  $S(Q)$  does not contain 1-bridges.*

*Proof.* Suppose  $S(Q)$  contains a 1-bridge  $\{e_0, e_1\}$ . The proposition just established implies that there is a free trace  $Y$  of an orientable surface with two vertices, intersecting both  $e_0$  and  $e_1$ . This is impossible, since by Theorem 5.12 both vertices of  $Y$  lie on the same edge.  $\square$

**Corollary 5.23.** *If  $Q$  be a brick, then every 2-bridge in  $S(Q)$  cuts off a component of one of the types shown in Fig. 5.*

*Proof.* Suppose  $S(Q)$  contains a 2-bridge. Proposition 5.21 implies that there is a free trace  $Y$  orthogonal to the bridge. Such a  $Y$  has 4 vertices and it is the trace of an orientable surface. Then one component of  $Q_Y$  is of one of the types admitted by Theorem 5.13, whose singular set is always of one of the types shown in Fig. 5.  $\square$

## 6 Bases of bricks for $n \leq 9$

We provide in this section a complete description of the bases of bricks  $\mathcal{B}_n$  for  $n \leq 9$  found by means of the algorithm described in Subsection 1.5. It is probably appropriate here to recall that  $\mathcal{B}_n$  was informally defined in Subsection 1.4 as the set of all bricks with  $n$  vertices, whereas the correct definition was given later in Section 3:  $\mathcal{B}_n$  is a set of representatives with respect to the equivalence relation generated by system-moves and assemblings of  $B_0$ . We can also eventually make precise a point which was only sketched in Subsection 1.5.

**Remark 6.1.** The set of moves employed in the algorithm described in Subsection 1.5 consists of all system moves of the kind  $T, MP, MP^{-1}$  through systems having at most one vertex more than the original system

We recall now that  $\mathcal{B}_n$  was split in Subsection 1.6 as  $\mathcal{B}_n^0 \sqcup \mathcal{B}_n^1$ , where  $\mathcal{B}_n^0$  consists of the elements of  $\mathcal{B}_n$  without length-1 loops. Before proceeding we prove here the result also stated in Subsection 1.6, according to which there exists a corresponding splitting of  $\mathcal{M}_n$  as  $\mathcal{M}_n^0 \sqcup \mathcal{M}_n^1$ .

*Proof of 1.10.* Let  $Q \in \mathcal{B}^0$  be a spine of a closed manifold  $M$ . If there were a spine  $Q'$  of  $M$  with less vertices than  $Q$ , this could be obtain from  $Q$  via a combination of disc-replacement moves. Since  $Q \in \mathcal{B}^0$  contains no length-1 loops, each such move would be a system-move: we get a contradiction, since  $Q$  is a brick. The manifold  $M$  must be irreducible since it has been proved in [4] that if a minimal spine of a closed manifold  $M$  is standard, then  $M$  is irreducible.  $\square$

We describe now  $\mathcal{B}_{\leq 9}^1$ , postponing  $\mathcal{B}_{\leq 9}^0$  for a moment, because to discuss it we will first need to introduce a new move on systems.

Our computations show that the set  $\cup_{n \leq 9} \mathcal{B}_n^1$  consists of 8 bricks  $B_0, \dots, B_8$ . The bricks  $B_0$ ,  $B_1$ , and  $B_2$  have already been considered above ( $B_1$  and  $B_2$  are shown in Fig. 40, and  $B_0$  was defined in Subsection 3.1). The bricks  $B_3$  and  $B_4$  are shown in Fig. 43, and the bricks  $B_5$ ,  $B_6$ ,  $B_7$  and  $B_8$  are shown respectively in Figures 44, 45, 46 and 47 (we always also show  $\mathcal{L}$  and the associated graph).

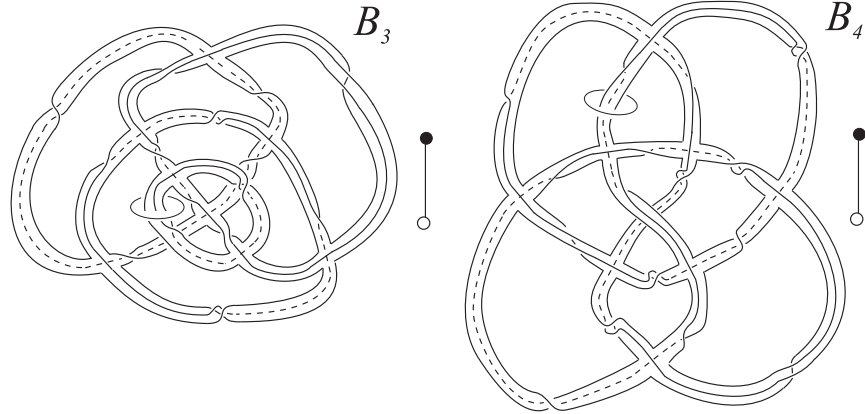


Figure 43: Description of  $B_3$  and  $B_4$ .

## 6.1 Twists

We introduce here a notion needed below to describe  $\mathcal{B}_{\leq 9}^0$ . Let  $Q$  be a quasi-standard spine of a manifold  $M$ , and let  $\gamma$  be a length-2 loop in  $Q$  such that  $\mathcal{R}(\gamma)$  is an annulus with 2 tongues. Let  $W$  be either the polyhedron shown in Fig. 27-right, or one of the polyhedra shown in Fig. 28. The boundaries  $\partial\mathcal{R}_Q(\gamma)$  and  $\partial W$  are homeomorphic. We can then choose a homeomorphism  $\psi : \partial W \rightarrow \partial\mathcal{R}_Q(\gamma)$  (there are 16 non-isotopic of them) and form a polyhedron  $Q' = \text{Cl}(Q \setminus \mathcal{R}(\gamma)) \cup_{\psi} W$ . Note now that  $W$  naturally sits in a solid torus  $H$ , with  $\partial W = W \cap \partial H$ .

**Proposition 6.2.** *The homeomorphism  $\psi : \partial W \rightarrow \partial\mathcal{R}_Q(\gamma)$  can be chosen so that it extends to a homeomorphism  $\tilde{\psi} : \partial H \rightarrow \partial\mathcal{R}_M(\gamma)$ . For these choices  $Q'$  is the spine of the Dehn surgered manifold  $M' = \text{Cl}(M \setminus \mathcal{R}_M(\gamma)) \cup_{\tilde{\psi}} H$ .*

*Proof.* The first assertion is easy and taken for granted. By construction  $Q'$  sits in  $M'$ , and we only need to show that  $M' \setminus Q'$  is an open 3-ball. To this end we note that  $M \setminus \text{Cl}(Q \cup \mathcal{R}_M(\gamma))$  is a ball  $B$ . Moreover  $\partial H \setminus \partial W$  consists of two discs  $D'$  and  $D''$ , and  $H \setminus (\partial H \cup W)$  consists of two balls  $B'$  and  $B''$ , with  $\text{Cl}(B') \cap \partial H = \text{Cl}(D')$  and  $\text{Cl}(B'') \cap \partial H = \text{Cl}(D'')$ . So  $M' \setminus Q' = B \cup_{\tilde{\psi}|_{D'}} B' \cup_{\tilde{\psi}|_{D''}} B''$  is a ball.  $\square$

We say that  $Q'$  is obtained from  $Q$  by *twisting* along  $\gamma$  with  $W$ . If  $W$  is a polyhedron as in Fig. 28 with  $v \geq 1$  vertices, we say that  $Q'$  is obtained from  $Q$  by  $v$ -*twisting*; we adopt the convention that making a 0-twist means leaving  $Q$  unaffected.

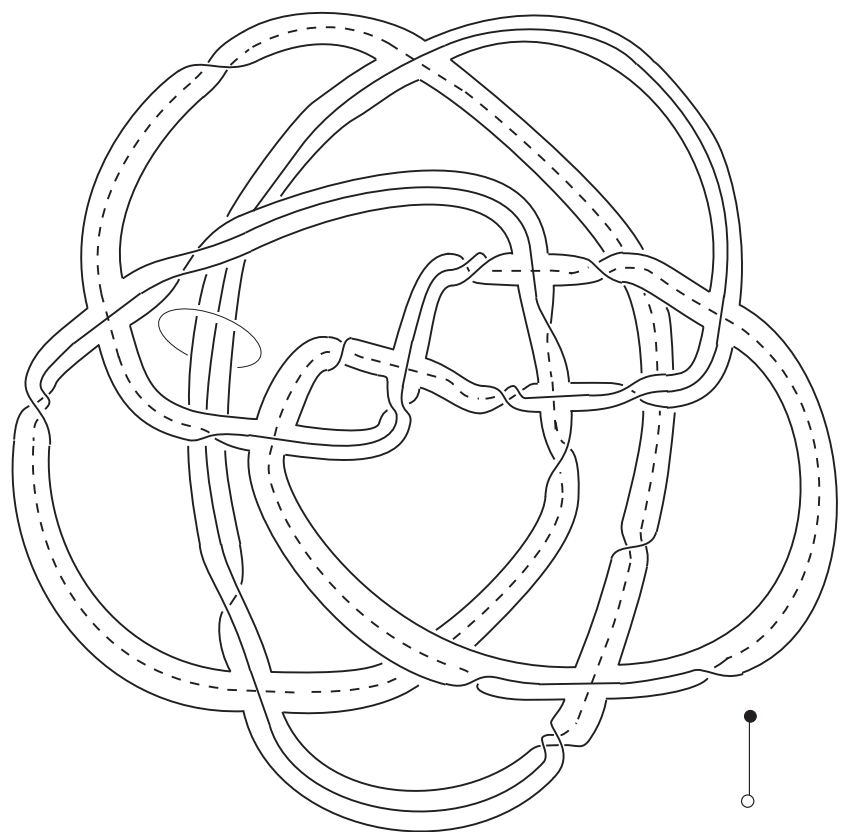


Figure 44: Description of  $B_5$ .

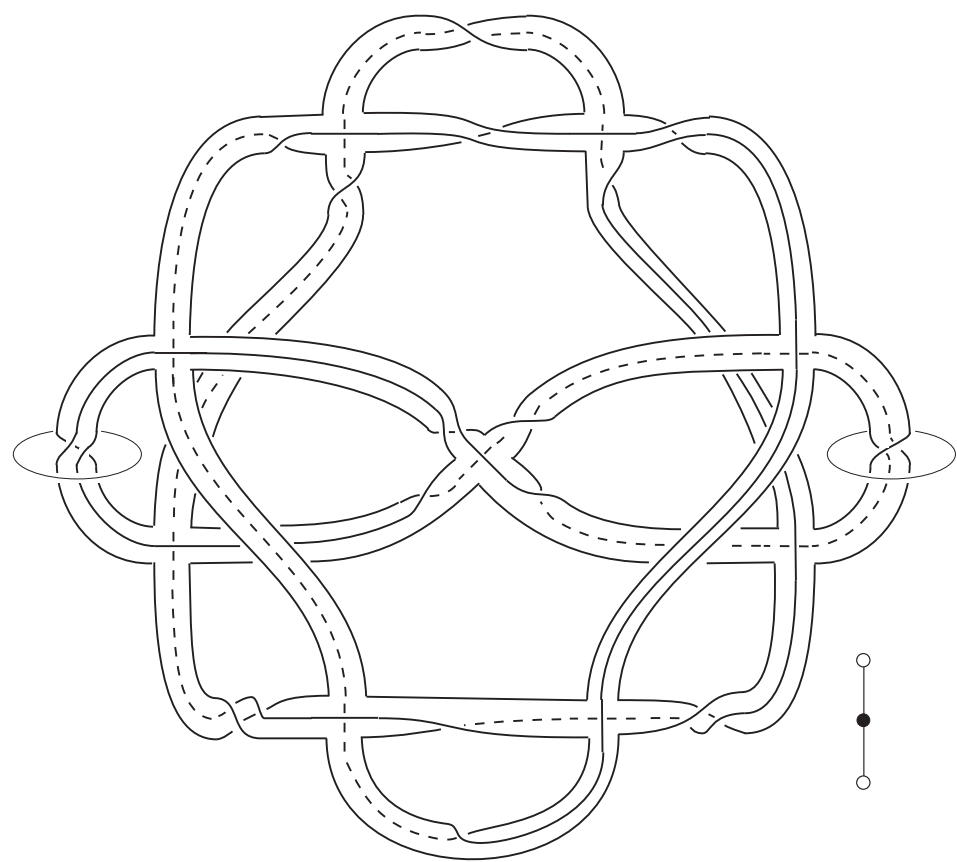


Figure 45: Description of  $B_6$ .

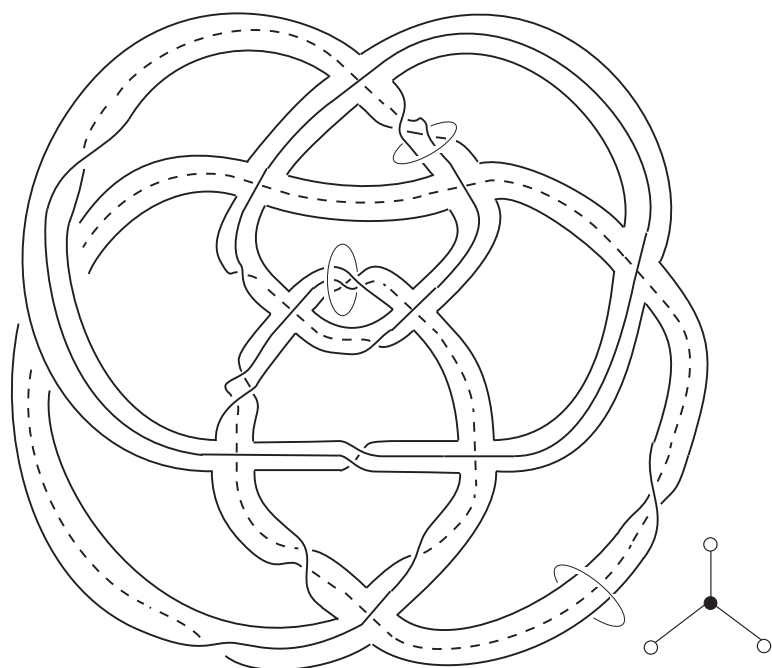


Figure 46: Description of  $B_7$ .

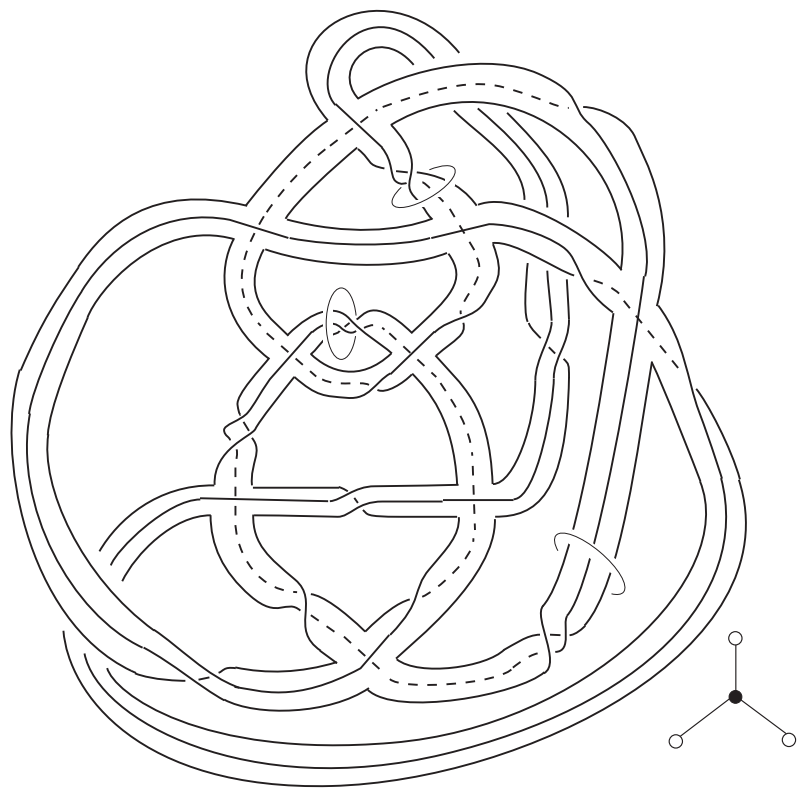


Figure 47: Description of  $B_8$ .

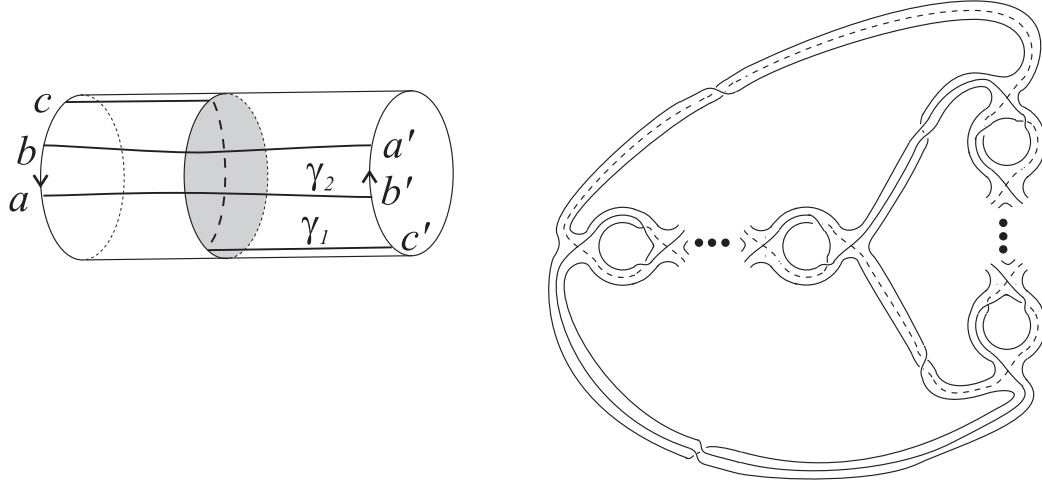


Figure 48: Two length-2 loops  $\gamma_1, \gamma_2$  in  $B'_0$  and the spine  $C_{i,j}$ .

## 6.2 The set $\mathcal{B}_n^0$ for $n \leq 9$

Our computations show that the set  $\cup_{n \leq 9} \mathcal{B}_n^0$  consists of 19 spines, which actually belong to the union of two classes  $\{C_{i,j}\}$  and  $\{E_k\}$ , which we now describe.

The polyhedron  $B'_0$  already considered above is a spine of  $S^2 \times S^1$  and it contains 2 length-2 loops  $\gamma_1$  and  $\gamma_2$ , shown in Fig. 48-left, such that  $\text{Cl}(S^2 \times S^1 \setminus \mathcal{R}_{S^2 \times S^1}(\gamma_1 \cup \gamma_2)) \cong (A, (2, 1))$  (where  $A$  is an annulus). Both  $\mathcal{R}_{B'_0}(\gamma_i)$  are annuli with two tongues on different sides; we can therefore perform a  $v_i$ -twist along each  $\gamma_i$  for  $v_1, v_2 \geq 0$ . If we do this with an appropriate gluing map we get the spine shown in Fig. 48-right, which we denote by  $C_{v_1, v_2}$ . Each  $C_{v_1, v_2}$  turns out to be a spine of the Seifert manifold  $(S^2, (2, 1), (1+i, 1), (1+j, 1), (1, -1))$ . We have  $B_1 = C_{1,0}$  and  $C_{i,j} = C_{j,i}$  for all  $i, j$ .

Poincaré's homology sphere  $(S^2, (2, 1), (3, 1), (5, 1), (1, -1))$  has a unique minimal spine  $E_0$  (Fig. 49-left). For any pair of non-adjacent edges of  $S(E_0)$  there is a length-2 loop  $\gamma$  intersecting them, isotopic to the singular fiber  $(5, 1)$ . Since  $\mathcal{R}(\gamma)$  is an annulus with two tongues, we can perform a  $v$ -twist along  $\gamma$ . If we do this with an appropriate gluing map we get the spine shown in Fig. 49-right, which we denote by  $E_v$ . Each  $E_v$  turns out to be a spine of  $(S^2, (2, 1), (3, 1), (5+v, 1), (1, -1))$ . It is worth mentioning that the brick  $B_3$  is also obtained from  $E_0$  by twisting along  $\gamma$ , but with the polyhedron in Fig. 27-right.

The set  $\cup_{n \leq 9} \mathcal{B}_n^0$  consists of all spines  $C_{i,j}, E_v$  with  $v \geq 0$  and  $i \geq j \geq 1$  having at most 9 vertices (i.e. with  $v \leq 4, i+j \leq 9$ ), except the cases  $v = 1$  and  $(i \geq 4, j = 2)$ . The spine  $E_1$  is indeed minimal, but it is not a brick: it contains two non-loop-

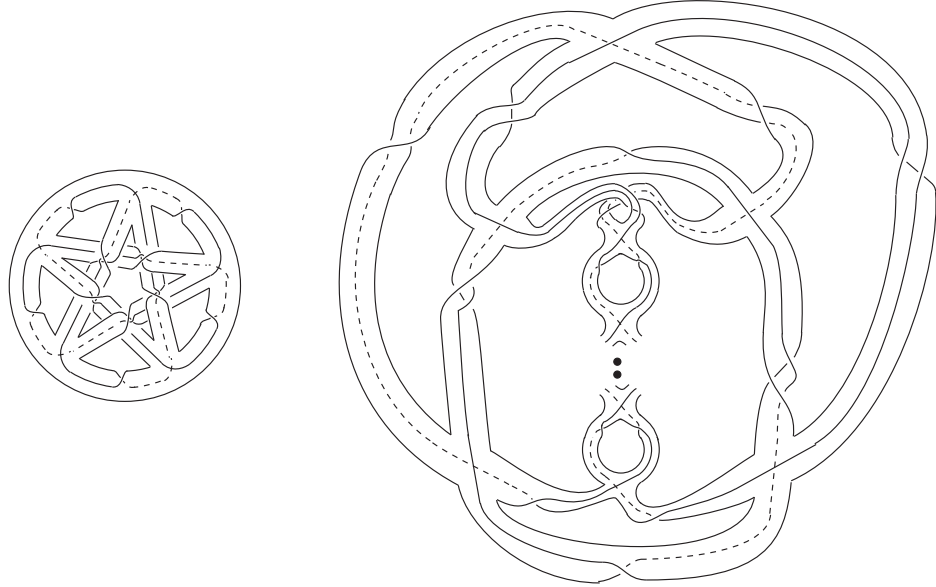


Figure 49: The spines  $E_0$  and  $E_k$ .

like toric triods and it belongs to  $\langle B_0 \rangle_{\text{self}}$ . This is coherent with the well-known fact that  $(S^2, (2, 1), (3, 1), (6, 1))$  fibers over  $S^1$  with torus fiber. Each  $C_{i,0}$  is minimal (for  $i \leq 9$ ), but it is contained in  $\langle B_0, B_1 \rangle_{\text{non-self}}$ . Each  $C_{i,2}$  for  $i \geq 4$  is not minimal, since  $E_{i-4}$  is a spine of the same manifold  $(S^2, (2, 1), (3, 1), (i, 1), (1, -1))$  with one vertex less.

## References

- [1] R. BENEDETTI – C. PETRONIO, *A finite graphic calculus for 3-manifolds*. Manuscripta math. **88** (1995), 291-310.
- [2] P. J. CALLAHAN – M. V. HILDEBRAND – J. R. WEEKS, *A census of cusped hyperbolic 3-manifolds*. Mathematics of Computation **68**:225 (1999), 321-332.
- [3] S. V. MATVEEV - A. T. FOMENKO, *Constant energy surfaces of Hamiltonian systems, enumeration of three-dimensional manifolds in increasing order of complexity, and computation of volumes of closed hyperbolic manifolds*. Russ. Math. Surv. **43** (1988), 3-25.

- [4] S. V. MATVEEV, *Complexity theory of three-dimensional manifolds*. Acta Applicandae Mathematicae **19** (1990), 101-130.
- [5] S. V. MATVEEV, *Tables of 3-manifolds up to complexity 6*. Chelyabinsk University Preprint, 1998.
- [6] S. V. MATVEEV, *Computer recognition of three-manifolds*. Experimental Mathematics **7:2** (1998), 153-161.
- [7] M. OVCHINNIKOV, *A table of closed orientable irreducible 3-manifolds of complexity 7*. Chelyabinsk University Preprint, 1997.